European Facility for Airborne Research Training Course
Exploring Air-Sea Interaction via Airborne Measurements
25 June - 4 July 2017, Shannon Ireland

Research flight by Group 4

Hanna Lokys[1], Jakub L. Nowak[2], Lichuan Wu[3], Pamela Trisolino[4], and Ana Álvarez Piedehierro[5]
Supervisor: Francesco Cairo[6]

1. University of Münster, Institute of Landscape Ecology, Münster, Germany, hanna.lokys@uni-muenster.de
2. University of Warsaw, Institute of Geophysics, Poland; jnowak@igf.fuw.edu.pl
3. Uppsala University, Uppsala, Sweden; lichuan.wu@geo.uu.se
4. Tuscia University and ENEA, Rome, Italy; pamela.trisolino@enea.it
5. University of Extremadura, Department of Physics, Badajoz, Spain; piedehierro@unex.es
6. Institute of Atmospheric Sciences and Climate, CNR; f.cairo@isac.cnr.it

EASI SCIENTIFIC REPORT

Differences between adjacent marine and terrestrial atmospheric boundary layer: thermodynamics and cloud microphysics

Jakub L. Nowak[1], Ana Álvarez Piedehierro[2]

1. University of Warsaw, Institute of Geophysics, Poland; jnowak@igf.fuw.edu.pl
2. University of Extremadura, Department of Physics, Badajoz, Spain; piedehierro@unex.es

1. INTRODUCTION AND AIM OF THE EXPERIMENT

Atmospheric boundary layer (ABL) is the lowest part of the troposphere, which is affected by diurnal cycle and where most of the weather phenomena occur. Its structure and properties are directly influenced by underlying surface, be it either sea or land with its topography and vegetation. Since the goal of the training course was to explore air-sea interaction via airborne measurements, one of the research flights was dedicated to study differences between ABLs which differs in the character of the surface underneath, i.e. between adjacent terrestrial and marine ABL.

The present report is focused on analysing those differences in terms of dynamics, thermodynamics and cloud microphysics. The structure of the document is the following. First, experimental site and intended flight strategy is described. In Section 4, we report the weather conditions encountered and present resulting actual final flight pattern. Overview of the instruments used and details of data processing is given in Section 5. Section 6 explains our methodology applied to compare sampled marine and terrestrial parts of the boundary layer. The tasks is approached from the two points of view - with focus on vertical structure and horizontal transitions as passing the coastline. The results obtained are showed and discussed in Section 7. Finally, conclusions concerning the flight and identified features are made.

2. DESCRIPTION OF THE TEST SITE

During the training course the aircraft was based at Shannon airport, one of the major airports in Ireland, located close to the west coast of the island (52°42′07″N, 8°55′29″W). Northeast from this site, there is a unique Mace Head Atmospheric Research Station, located directly at the coast on a Mace Head peninsula (53° 19' 33'' N, 9° 53' 58'' W), northwest from Shannon. It is operated by National University of Ireland, Galway, and performs regular measurements of aerosols, trace gases and meteorological conditions. Since the wind exposure is primarily westerly, clean background conditions over North Atlantic ocean can be studied without influence of continental emissions. The nearest major urban area is the ciity is Galway, 88 km east from the point. According to the data collected over years at the station, "*the climate is mild and moist, being dominated by maritime air masses. October to December are the wettest months, with April and May being the driest. Relative humidity is generally high, at about 80-85%. Average air temperature is about 10 degrees Celsius (~15 degrees Celsius in summer, ~5 degrees Celsius in winter). Sea temperature ranges from about 10 degrees Celsius in winter to about 15 degrees Celsius in summer. Sunshine is scarce, averaging 1290 hours per annum".*

Location of the both Shannon airport and Mace Head station is marked on a map below (red and yellow dots respectively). From the point of view of airborne experiment design, it is advisable to take advantage of the ground base and remote sensing routine measurements at the station, so it was decided to include horizontal legs overflying this location in the flight strategy.

Figure 1. Location of aircraft base - Shannon airport - and Mace Head Research Station

3. FLIGHT STRATEGY

In order to investigate differences between boundary layer over land and over ocean, the concept of flight pattern was proposed to include horizontal legs flown perpendicular to the coastline, half of the distance over land and half over the ocean. Preferably, those legs should overpass Mace Head observatory while crossing seashore, because the station is located exactly at the coast and can provide additional information about ground conditions and vertical structure of the atmosphere at this point. It was thus suggested to do 6 stacked legs between points E and F (see Figure 2) at different altitudes, which resulted in the following initial flight plan:

1. Take off EINN – Climb to 300 ft AGL.
2. Leg from EINN to point E at 300 ft AGL (40 nm – 14’).
3. Leg to point F at 300 ft AGL (60 nm – 20’).
4. Climb to 500 ft AGL (2’).
5. Leg to point E at 500 ft AGL (60 nm – 20’).
6. Climb to 700 ft AGL (2’).
7. Leg to point F at 700 ft AGL (60 nm – 20’).
8. Climb to 900 ft AGL (2’).
9. Leg to point E at 900 ft AGL (60 nm – 20’).
10. Climb to 1100 ft AGL (2’).
11. Leg to point F at 1100 ft AGL (60 nm – 20’).
12. Climb to 1500 ft AGL (2’).
13. Leg to point E at 1500 ft AGL (60 nm – 20’).
14. Leg back to EINN at 1500 ft AGL and landing (40 nm – 14’).

Flight duration : ~ 2h30

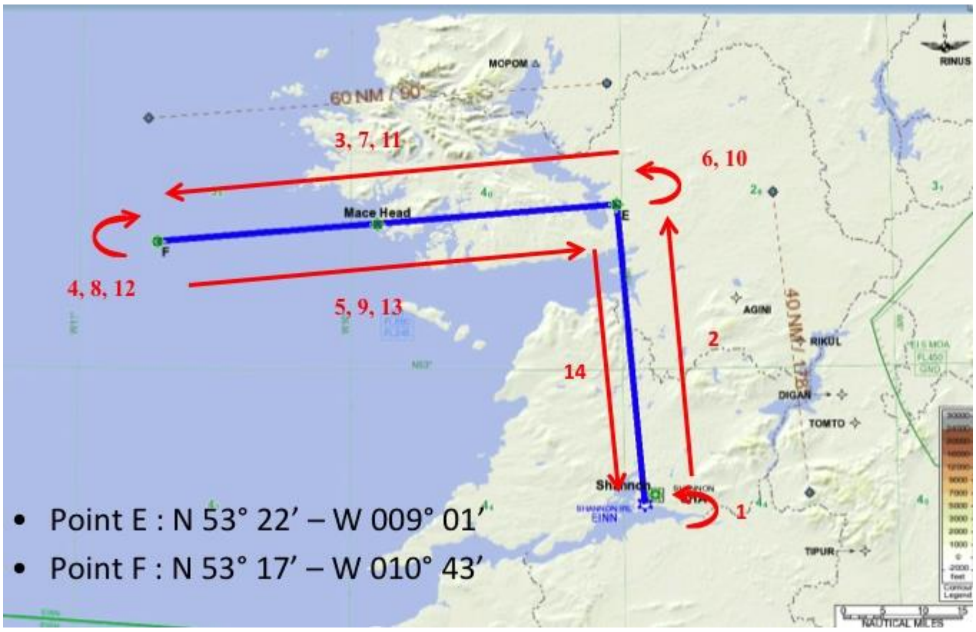

Figure 2. Suggested flight plan. Leg description above.

This conceptual flight plan was adopted, after discussing it with the pilots and the SAFIRE crew, to comply with local geographical conditions, safety regulations and airspace organization in the neighborhood of Shannon. It was decided to slightly lengthen the horizontal legs to be able to measure fluxes both over land and over sea. Moreover, a vertical profile should be included to study vertical structure, in particular to estimate the height of the boundary layer top. Finally, the agreement was reached on the following pattern: ferry out to target site and repeat 3 stacked legs within the ABL and one above; each leg should consist of 12 minutes over land and 12 minutes over sea, overpassing Mace Head. Particular levels will be decided according to vertical profile and visibility conditions, which limit the minimum possible height. Measurements should be taken with all the instruments onboard ATR, with LIDAR pointing up while flying inside the BL and turned down for the leg above the BL.

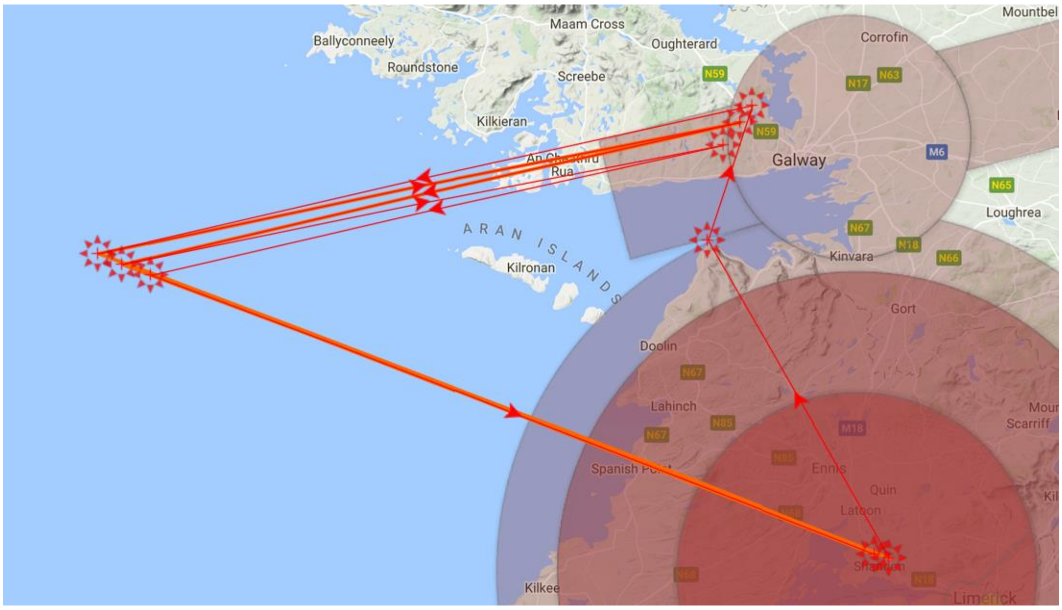

Figure 3. Final flight plan, including air traffic control zones.

Table 1. Final flight plan: segment description. Numbers as in figure 3 and 4.

Segment	Description
1	Exit Shannon ATC area via authorised exit point.
2	Transit to waypoint E.
3a	Profile to identify BL height. Decide heights for legs 4, 5, 6 and 7. Reaching minimum altitude over sea.
3b	Horizontal leg heading waypoint F at minimum altitude allowed over the sea.
4	Backward leg heading waypoint E at mininum altitude allowed over land.
5	Horizontal leg inside the ABL.
6	Horizontal leg inside the ABL.
7	Horizontal leg over the ABL.

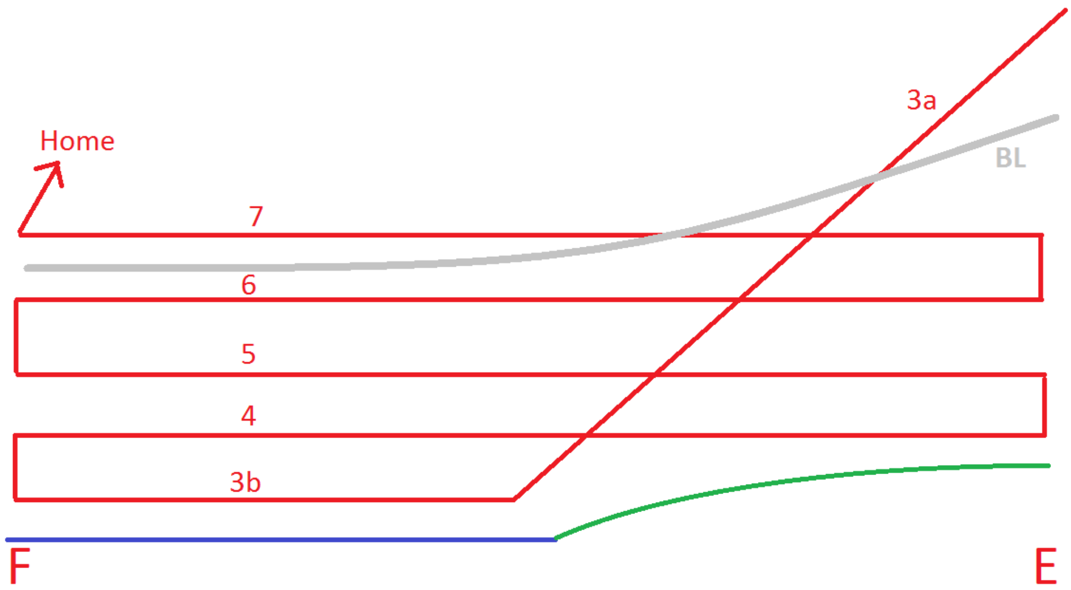

Figure 4. Final flight plan: vertical cross-section sketch.

The ATR aircraft offers several working station (WS) for scientists onboard to monitor different parameters and instruments. Therefore, the duties were distributed among the group members as following:

- General WS: Hanna Lokys (scientific leader)
- General WS: Lichuan Wu (monitor vertical structure)
- Chemistry WS: Ana Álvarez Piedehierro
- Microphysics WS: Jakub Nowak
- LIDAR WS: Pamela Trisolino

Figure 5. EASI Training School Group 4 with supervisor Francesco Cairo in front of the ATR42-SAFIRE aircraft before the research flight.

4. DESCRIPTION OF THE FLIGHT

According to the strategy described in the previous section, the details of the flight pattern, especially the exact levels of the horizontal legs, needed to be decided during the flight depending on the conditions encountered. Those refer to the general weather situation, cloudiness which might limit minimum possible flight level and vertical structure of the ABL.

4.1 WEATHER CONDITIONS

Weather forecast for 28 June 2017 predicted a low pressure system extending over much of Great Britain and Ireland with fronts around the experimental site (figure 6). Only weak wind was expected which is optimal to characterize the boundary layer over land and over ocean separately since the mixture between two air masses is minimized. Therefore, the flight of the group 4 was scheduled for this day. However, frontal systems, in particular the occluded one west from Ireland (see figure 7) developed quite thick cloud cover over significant area. The presence of clouds might force instrumental flight conditions which severely limits the minimum safe altitude. Then fulfilling the goal of penetrating ABL stands in question. The clouds were expected to move towards the area of the experiment and the ones already present there were likely to grow. Because of that it was decided to fly in the morning despite the ABL being usually well developed in the afternoon.
METAR issued shortly before take-off reported temperature 15°C, dew point 12°C, weak wind and two cloud layers (few at 1800 ft, scattered at 4000 ft). Shortly after landing air temperature was reported to be 17°C, dew point 11°C, weak wind as well but cloud cover increased (scattered at 2000 ft and broken at 4000 ft) which confirms our anxieties. Balloon sounding performed at noon at the Valentia station, southwest from Shannon, shows shallow warm surface layer (figure 8). The atmosphere seems to be well mixed up to 950 hPa which might be the height of the ABL. There is also a moderate capping inversion around 850 hPa.

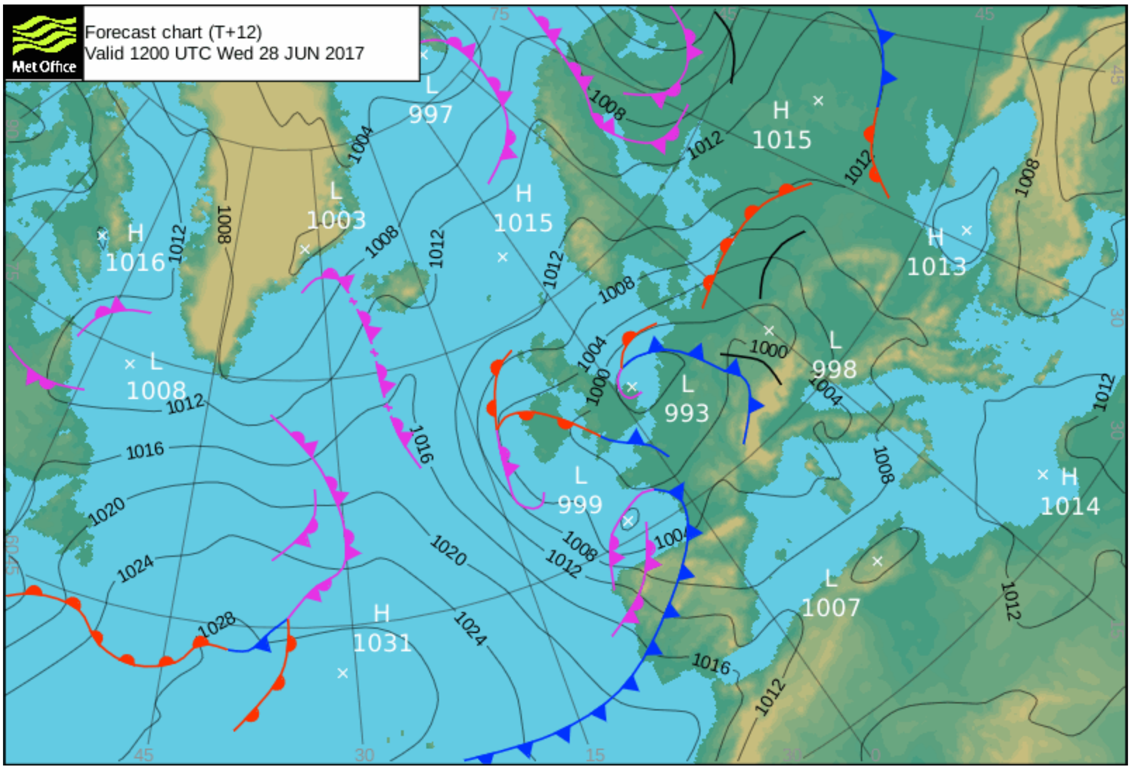

Figure 6. Surface pressure chart for 28 June 2017 12:00 UTC provided by Met Office.

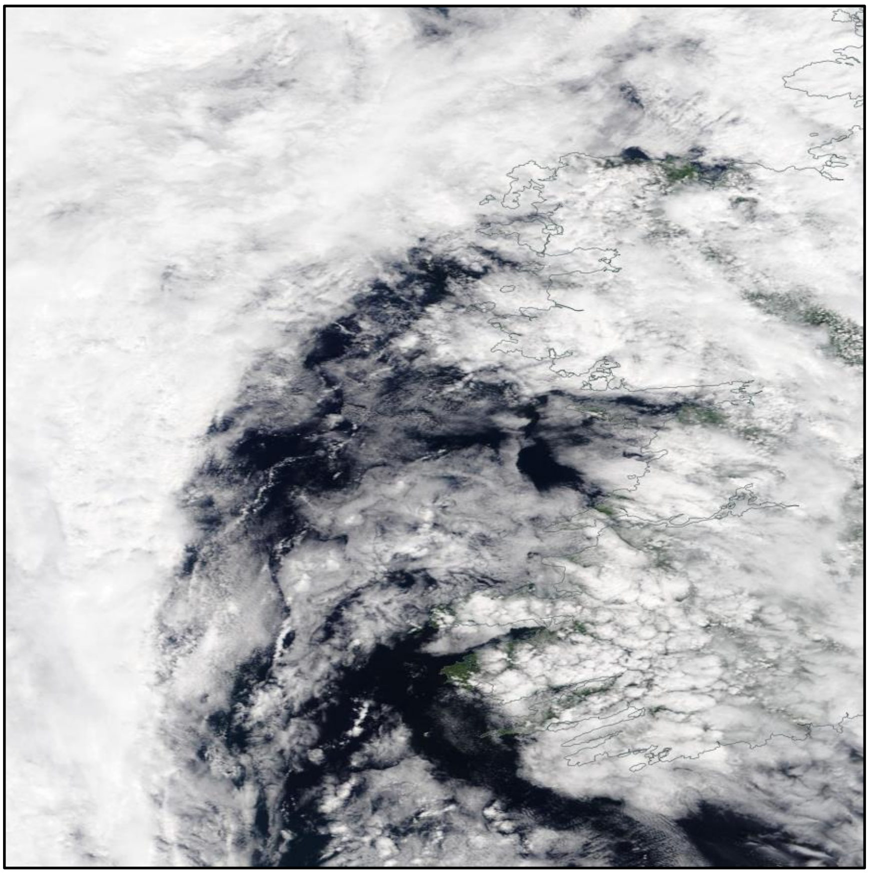

Figure 7. True color satellite image showing the west coast of Ireland (NASA MODIS Terra, 28 June 2017 ~12 UTC, 250 m resolution).

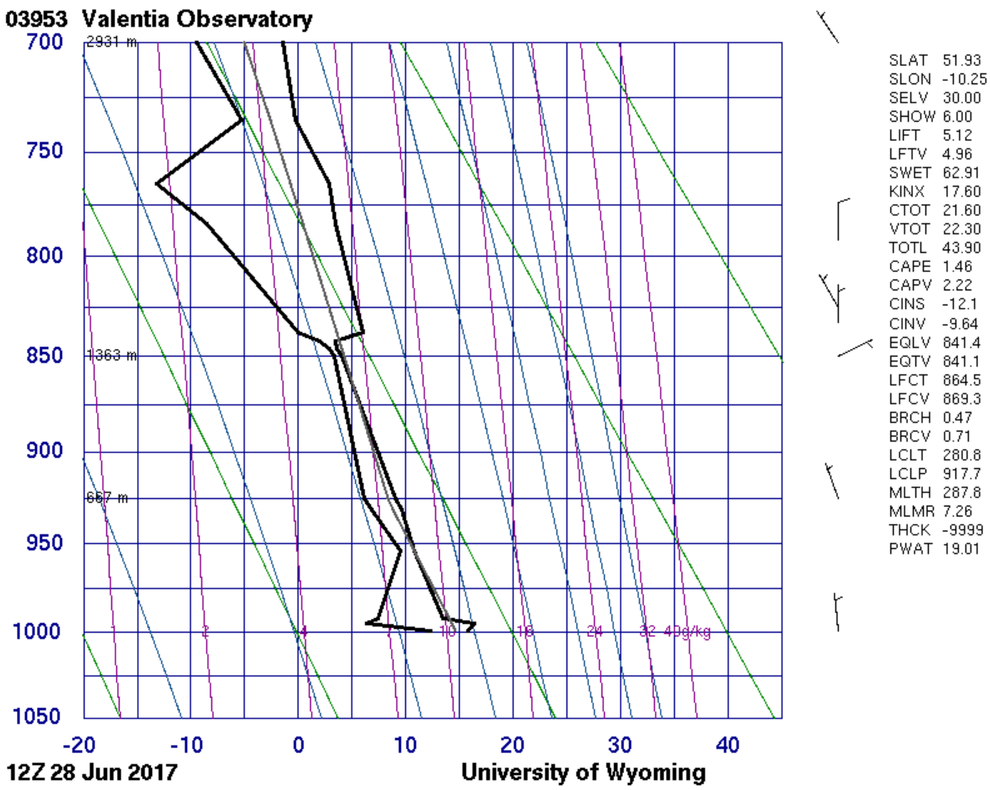

Figure 8. Sounding at Valentia Observatory (28 June 2017, 12 UTC).

4.2 ACTUAL FLIGHT PATTERN

Final flight track was determined by the exact weather conditions encountered. Due to clouds over land and its complex topography close to the coast, the minimum possible altitude was around 400 m. Over the ocean, we managed to fly at around 65 m above the surface thanks to good visibility. The main part of the flight were east-west horizontal legs. Finally, over ocean they were flown at roughly 65 m, 165 m, 405 m, 740 m and 1230 m, while over land at 405 m, 740 m and 1230 m. Unfortunately the first descending profile started after passing the shore, which forced the lowest ocean leg to be much shorter. In the end, another sounding and short leg over water surface was done on the way back to Shannon airport.

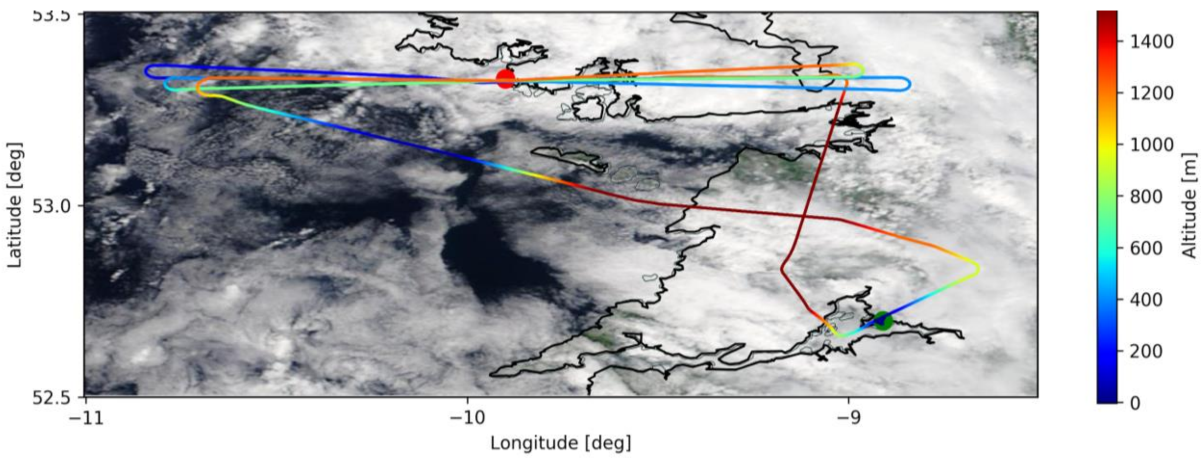

Figure 9. Flight track with color-coded altitude with respect to sea level drawn over true color satellite image (NASA MODIS Terra, 28 June 2017 ~12 UTC, 30 m resolution).

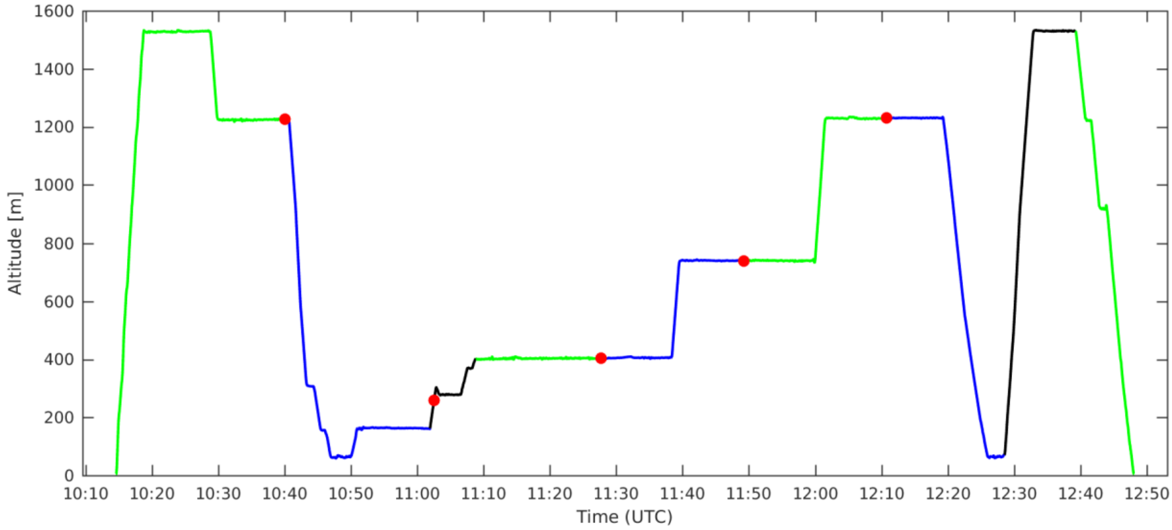

Figure 10. Flight pattern - altitude. Profiles and legs over land (green), profiles and legs over ocean (blue), mixed or ambiguous segments (black), overpassing Mace Head (red dots).

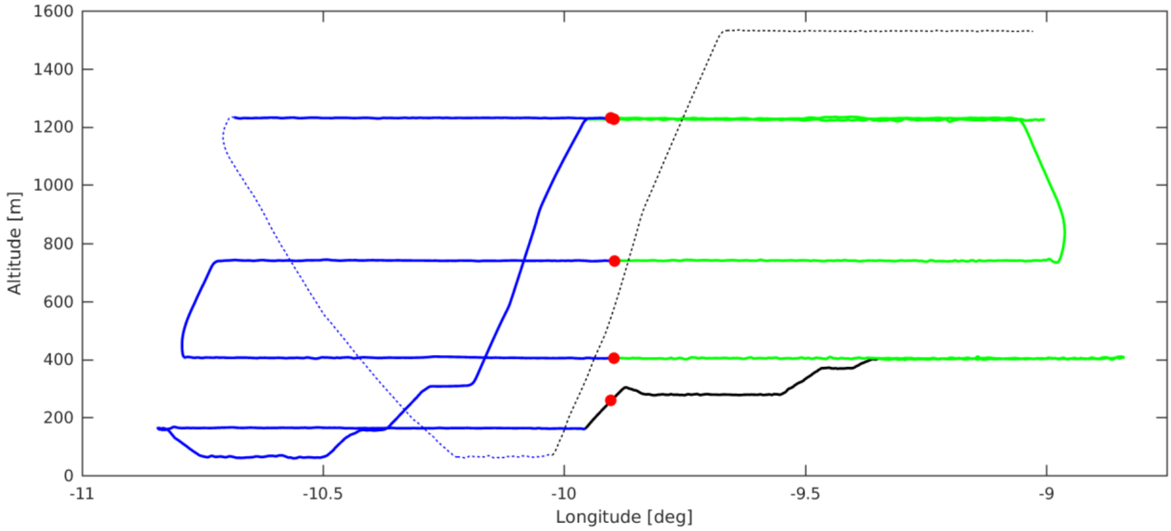

Figure 11. Flight pattern in vertical east-west plane. Colors same as in fig. 10. The way back to the airport lying outside this plane is marked with dashed line.

4.3 FLIGHT NOTES

Flight ID: 13	*June 28, 2017 (Local Time: 11 to 13:30)*
Take Off:	*10:13 28-Jun-2017 UTC (UTC = LT + 1:00)*
Touch Down:	*12:48 28-Jun-2017 UTC*
Flight Duration:	*2:35*
Flight Scientist:	*Hanna Lokys*

Table 2. Detailed flight notes.

Segment	Start time	End time	Altitude	Notes
Takeoff to WP1	10:05		0	Begin taxing
	10:13			Take off

	10:16		1500 m	Into a cloud CO_2 stable at 399 ppm CO 0.074 ppm CH_4 1.882 ppm O_3 31.2 ppb
	10:24			Above cloud
	10:26			Clouds above the aircraft
	10:27			Entering clouds
	10:28		1200 m	Descending to 4000 ft (1200 m) approaching beginning of the first leg. Cloud layer below us but not thick, maybe we can fly below.
Leg 1	**10:30**	**10:50**	**4000 ft Descent 200 ft**	**Going to MHO at 4000 ft and then descend to 200 ft to WP2 over sea**
	10:31		1240 m	Inside cloud. Heading to MHO at the same altitude
	10:36			Overpass MHO in three minutes and we will start descent. Fly below the cloud level in our way back
	10:39			Overpass MHO
	10:40			Start descent
	10:41		1000 m 3000 ft	No clouds. We will descend as much as we can. Sea state very calm
	10:43		1400 ft	LIDAR info: BL at 600-700m
	10:45		155 m	
	10:46		200 ft ~70 m	Flying low until WP2
	10:50		166 m	End of leg 1. Turning back
Leg 2	**10:52**	**11:14**	**500 ft - 1000 ft**	**From WP2 to WP1 500 ft over sea and 1000 ft over land**
	11:00		1000 ft	Climbing to 1000 ft above sea level
	11:01			Approaching the coastline, wind direction change
	11:14		1000 ft	End of leg 2, turning back LIDAR: BL 1000m (407 m)
Leg 3	**11:16**	**11:37**	**1000 ft**	**From WP1 to WP2, 1000 ft above sea level**
	11:21			Raining, closed cloud cover over the aircraft over land
	11:25			Coastline; ~ 20 Wm^{-2} upward global radiation (over the sea) ~ 42 Wm^{-2} upward global radiation (over the land)
	11:27			Over water, few clouds (scattered); overpass MHO
	11:33			Clouds at aircraft height (scattered)

	11:35			LIDAR: BL 1000m , clouds 1200m
	11:37			End leg 3, turning back, LIDAR turned towards the ground
Leg 4	**11:39**	**11:59**	**2400 ft**	**From WP2 to WP1, 2400 ft above sea level**
	11:48			coastline
	11:49		2400 ft	Shortly into the clouds. Overpassing MHO, we will keep going at 2400 ft over land.
	11:57			Right at the bottom of the clouds (in-out)
	11:59			End of leg 4, turning back We are above clouds
Leg 5	**12:00**	**12:18**	**4000ft**	**From WP1 to WP2, 4000 ft above sea level**
	12:00			Calibrating PICARRO
	12:04			Scattered clouds below and above
	12:07			No clouds.
	12:08			Inside clouds
	12:09			Overpass MHO
	12:10			In cloud but over the sea
	12:15			“Surfing” at the top of the cloud. We have picture
	12:18			End of leg 5, turn towards Shannon airport (entry to cylinder at ERABI)
Sounding	**12:20**	**12:24**	**4000 ft - 200 ft**	**Sounding on the way back to the airport**
	12:23			Crossing scattered clouds
Flight back	**12:24**		**200 ft - 5000 ft - ground**	**Flight as low as possible until the entry cylinder of Shannon airport**
	12:25		200 ft	Turn the LIDAR upward, so we can see the PBL at 600 m. Flying this low for a few minutes
	12:28			End of the low flight, still very calm sea
	12:31		1300 m	Turn the LIDAR downward
	12:32			Start descent
	12:33			End of Picarro measurements
	12:42			Lidar window closed
	12:45			Restart LIDAR and turn upward
Landing	**12:48**			**plaNet altitude (GPS) 19m**
On ground				**Few LIDAR measurements; BL at 600-700 m.**


Figure 12.a.10:05:11, taxi.


Figure 12.b.10:24:32.


Figure 12.c.10:25:55.


Figure 12.d.10:46:34 200ft over sea.


Figure 12.e.10:57:17.


Figure 12.f.11:04:48 over MHO area.


Figure 12.g.11:08:26.


Figure 12.f.11:25:50.


Figure 12.i.11:25:53.

 *Figure 12.j.11:26:14.*	 *Figure 12.k.11:27:20 Over MHO area.*	 *Figure 12.l.11:29:03.*
 *Figure 12.m.11:36:31.*	 *Figure 12.n.11:41:01.*	 *Figure 12.o.11:41:35.*
 *Figure 12.p.12:02:27.*	 *Figure 12.q.12:16:03.*	 *Figure 12.r.12:20:42.*

Figure 12. Pictures taken during the research flight.

5. INSTRUMENTATION AND MEASUREMENTS

Measurements analysed in the present report were taken with the research aircraft ATR42-320, operated by SAFIRE, a division of Meteo-France. The platform is aimed at investigating the troposphere and was adapted to hold a wide range of instruments which allow to study dynamics, thermodynamics, radiation, microphysics and chemistry. Typical true air speed is 100 m/s while minimum altitude resulting from safety regulations is 200 ft over sea and 500 ft over land. The crew include 2 pilots, 2 flight engineers and up to 7 scientists.

Platform position

Aircraft position in Earth frame of reference, including altitude, latitude and longitude was measured with inertial navigation system and GPS unit.

Pressure and wind

Several Pitot tubes are installed close to the nose of the aircraft. They allow to measure total and static pressure. From them, one can also get information about true airspeed. Three components of the flow velocity were measured with a classic five-hole pressure probe. The local total and static pressure is sampled at 5 different locations. Such information can be used to obtain air speed and aircraft orientation in space (Euler angles). Correcting for the platform motion, wind velocity is calculated in Earth frame of reference.

Temperature

Air temperature was measured with Rosemount probes. The housing protects the sensing wire from dirt, sand and droplets. In present study, temperature data from non-deiced Rosemount thermometer was taken for further analysis. Since the aim was to investigate mostly boundary layer, flight level was limited to around 2 km and thus severe icing was not expected but additional heating of the thermometer housing might slightly affect the temperature readings.

Humidity

Air humidity was measured with two different instruments onboard. Relative humidity is obtained with a capacitance sensor (Humaero). Unfortunately, some indications of strong wetting was observed during signal inspection. Inside the clouds, in their neighbourhood and sometimes for quite a long time after leaving the cloud, the results seem to be unrealistic (RH up to 130 %). Thus, the data from this instrument was rejected.

The second device is Licor Li7500 which measures absorption of infrared radiation due to water vapor molecules. Absorbed fraction depends on the concentration of absorbing particles. Therefore, it can be converted to absolute humidity reported in g/m3. Licor is an open-path instrument, so not only clear air containing water vapor enters the sampling volume but also liquid and solid particles, especially cloud droplets. Indeed, inside the cloud the readings are completely unreliable due to absorption by droplets.

Nevertheless, we decided to use humidity data from Licor but the record was corrected in the cloudy parts. Namely, in ‘cloudy’ time periods, i.e. those when liquid water content (LWC) measured with Gerber’s Particle Volume Meter was higher than 0.05 g/m3, humidity values were replaced with levels corresponding to saturation at given temperature (taken from Rosemount thermometer). Absolute humidity can then be converted to relative one with known formulas. The example cloud penetration and result of the correction procedure for both relative and absolute humidity is shown in the figures below.

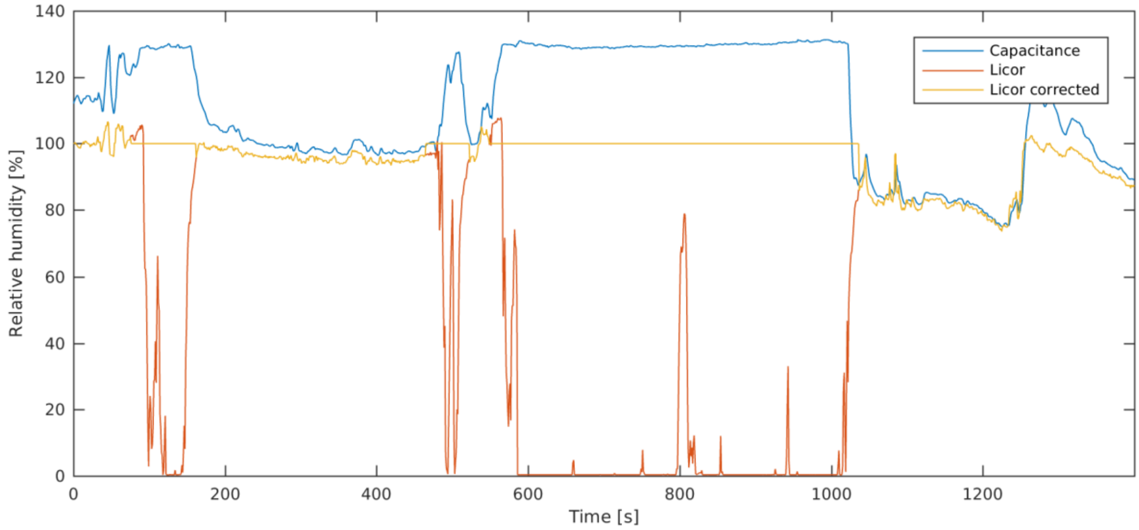

Figure 13. Relative humidity during cloud penetration: signals from capacitance sensor, Licor and final corrected humidity record.

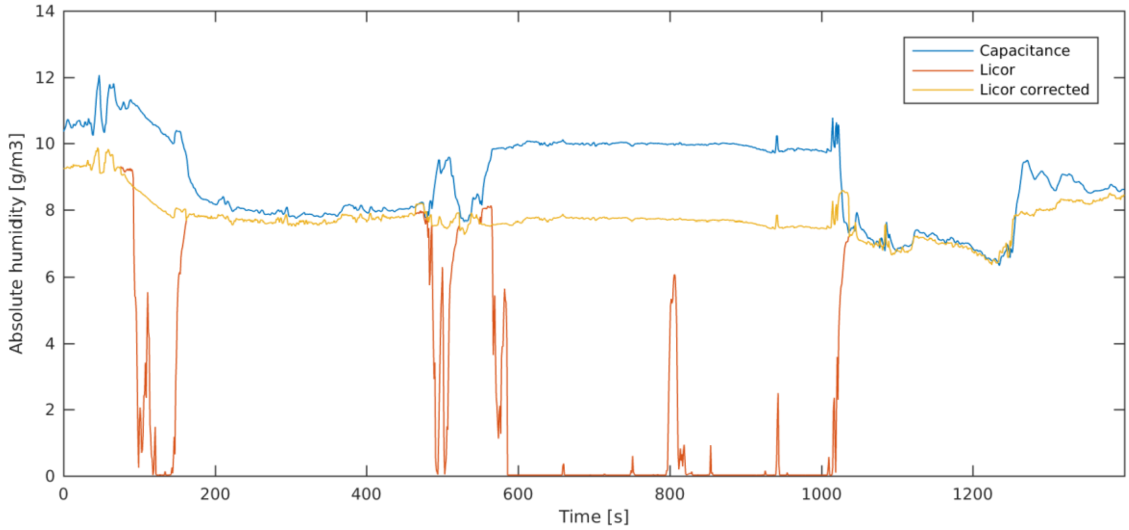

Figure 14. Absolute humidity during cloud penetration: signals from capacitance sensor, Licor and final corrected humidity record.

<u>Cloud microphysics</u>

Total liquid water content was measured with Gerber probe (Particle Volume Meter). The instrument estimates total volume and total surface of a sample of cloud droplets based on amount of laser radiation scattered on them. Individual droplet sizes were measured with DMT Cloud Droplet Probe. This device is based on Mie scattering of thin laser beam by a single droplet. Thus, the sampling volume is tiny but the data about the droplets entering it can be integrated over time to built the whole size distribution in the range between 2 and 50 microns. Summing up all the size bins, total number concentration and LWC can be calculated. Results show very good agreement between PVM and CDP in terms of liquid water (see the figure below). However, there is probably a major error in total surface and resulting mean effective diameter given by PVM and those variables have been rejected.

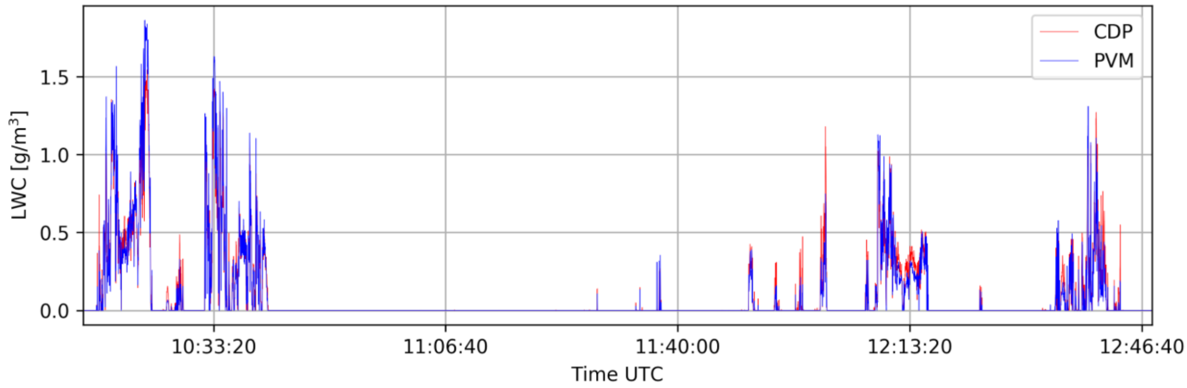

Figure 15. Liquid water content during the whole flight measured with CDP and PVM.

6. METHODOLOGY

The whole flight was separated into segments based on the position in space (i.e. altitude, latitude and longitude). In total, 24 segments were identified (listed in the table below). There are 2 types of them - horizontal legs and vertical profiles or steps. Here we adopt the convention that 'profile' is a sounding which includes most of the height range in the flight, covers at least the boundary layer and provides general information about vertical structure in the atmosphere. 'Step' is a transition between two consecutive horizontal legs. Each segment can be flown over specified surface - land or ocean. In case it covers both types or the distinction is difficult because of the complex shape of the coastline and non-trivial topography (hills, small bays and lakes) the segment is classified as mixed. Such segmentation results in simplified flight pattern (figure 16) and allows for systematic analysis of the respective parts.

Table 3. Flight segments.

#	Start	End	Duration	Height [m]		Type	Surface	Name
1	10:14:33	10:18:44	4:11	5	1529	ver	land	prof_land1
2	10:18:44	10:28:45	10:01	1529	1529	hor	land	leg_land1
3	10:28:45	10:29:59	1:14	1529	1225	ver	land	step_down 1
4	10:29:59	10:40:37	10:38	1225	1225	hor	land	leg_land2
5	10:40:37	10:46:59	6:22	1225	64	ver	ocean	prof_oce1
6	10:46:59	10:49:57	2:58	64	64	hor	ocean	leg_oce1
7	10:49:57	10:50:59	1:02	64	163	ver	ocean	step_up1
8	10:50:59	11:01:55	10:56	163	163	hor	ocean	leg_oce2
9	11:01:55	11:03:17	1:22	163	279	ver	mixed	step_up2
10	11:03:17	11:06:35	3:18	279	279	hor	mixed	leg_mix1
11	11:06:35	11:08:52	2:17	279	406	ver	mixed	step_up3
12	11:08:52	11:27:45	18:53	406	406	hor	land	leg_land3
13	11:27:45	11:38:21	10:36	406	406	hor	ocean	leg_oce3

14	11:38:21	11:39:41	1:20	406	741	ver	ocean	step_up4
15	11:39:41	11:49:11	9:30	741	741	hor	ocean	leg_oce4
16	11:49:11	11:59:58	10:47	741	741	hor	land	leg_land4
17	11:59:58	12:01:40	1:42	741	1231	ver	land	step_up5
18	12:01:40	12:10:46	9:06	1231	1231	hor	land	leg_land5
19	12:10:46	12:19:09	8:23	1231	1231	hor	ocean	leg_oce5
20	12:19:09	12:26:03	6:54	1231	65	ver	ocean	prof_oce2
21	12:26:03	12:28:32	2:29	65	65	hor	ocean	leg_oce6
22	12:28:32	12:33:00	4:28	65	1531	ver	mixed	prof_mix1
23	12:33:00	12:39:12	6:12	1531	1531	hor	mixed	leg_mix2
24	12:39:12	12:48:05	8:53	1531	5	ver	land	prof_land2

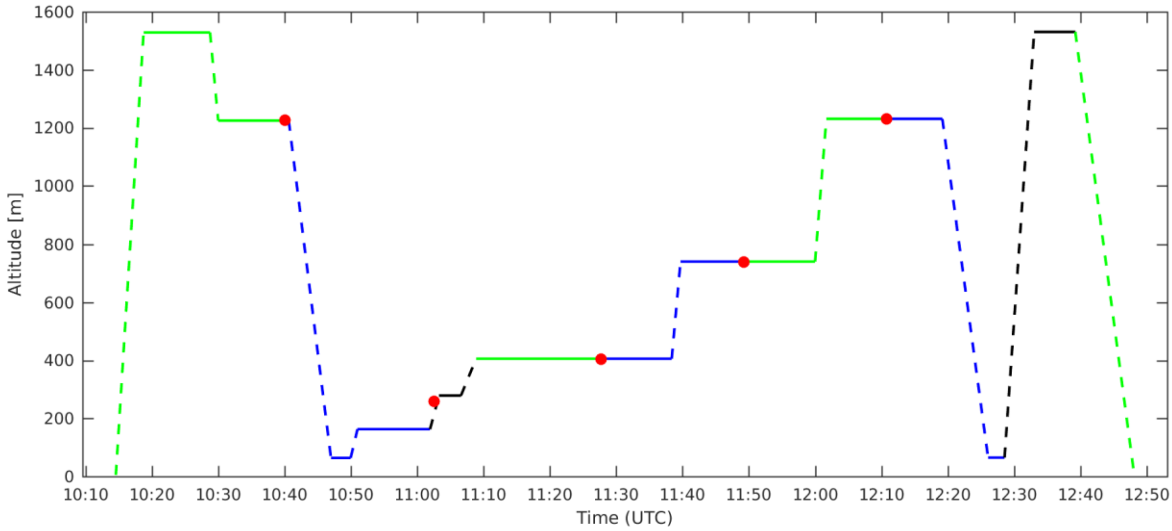

Figure 16. Flight vertical pattern simplified according to the segmentation. Horizontal legs (solid) and vertical profiles (dashed) over land (green) and ocean (blue) or mixed surface (black) together with overpassing Mace Head (red dots).

Firstly, the vertical structure of the lower part of the atmosphere in two locations (ocean, land) in two moments in time (at the beginning and at the end of the flight) was studied in terms of dynamics (wind, turbulent kinetic energy) and thermodynamics (potential temperature, humidity). For this purpose, segments 1 (prof_land1), 5 (prof_oce1), 20 (prof_oce2), 24 (prof_land2) were used. Based on those profiles, one can describe stability and identify different sublayers, including ABL. None two out of the selected four flight parts were flown exactly in the same point or with the same path. But if at least local horizontal homogeneity is assumed, the evolution of the vertical structure in time can be described by qualitative comparison of the soundings taken at the beginning and at the end of the flight.
In the second stage, horizontal legs are studied in terms of the same physical quantities. The objective is to find differences/similarities between the ones flown over sea and those over land. Particularly interesting are adjacent segments at the same level for which one can try to look for a transition between the zones of different characteristics.

Thermodynamic records are supported with cloud microphysics data. The presence of cloud is marked by non-zero liquid water content. PVM signal can be used as a proxy to find cloud penetrations (see figure 17). Additionally, droplet size distribution and total number concentration is calculated based on the CDP data.

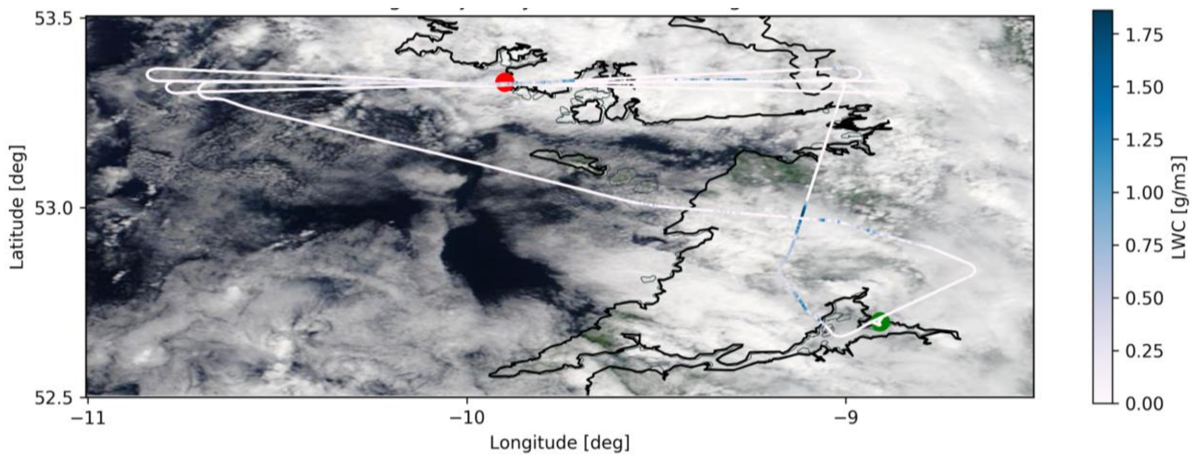

Figure 17. Flight track with color-coded liquid water content (reported by PVM) drawn over true color satellite image (NASA MODIS Terra, 28 June 2017 ~12 UTC, 30 m resolution).

7. RESULTS

7.1. VERTICAL STRUCTURE OF THE ATMOSPHERE

7.1.1. Continental

Take-off, segment 1

First vertical profile over land taken just after take-off show the presence of three main layers in the penetrated part of the troposphere:

1. Well-mixed layer extending from the ground up to around 300 m. Nearly constant potential temperature indicates neutral stability. Horizontal wind also does not change much with height. There are two local maxima of turbulent kinetic energy: first at the ground connected with turbulence generation by friction, below the top of the layer. The latter is probably the result of the convection developing inside the layer. Mixing slowly homogenizes vertical gradients. One can also spot slight wind shear at the top. All those facts suggest this is actually the boundary layer. It is not very deep yet, partly because the sun rose less than 3 hours before and partly due to considerable cloud cover which inhibits the production of daytime convection.
2. Intermediate stable layer extending up to roughly 900 m, i.e. up to the cloud base. Potential temperature grows gently with height, almost linearly. Horizontal wind is approximately constant, except the shear at the bottom border with the former layer and at the top.
3. Cloud layer of complex structure. Liquid water content does not increase monotonically with height, which means the cloud is not a result of a simple convective motion of a parcel rising up and expanding in the atmosphere. The cloud field might consist of independent layers (not only one thick cloud penetrated) or the situation was horizontally inhomogeneous. Major droplet size seems to be constant while the spread of the distribution grows with altitude. Mean horizontal wind is close

two zero but large fluctuations can be observed. There are two maxima in TKE which nicely correspond with regions of highest LWC. The gradient of potential temperature higher than in the layer below and clear difference in horizontal wind suggest that the cloud layer is decoupled from the bottom and might have been advected from elsewhere.

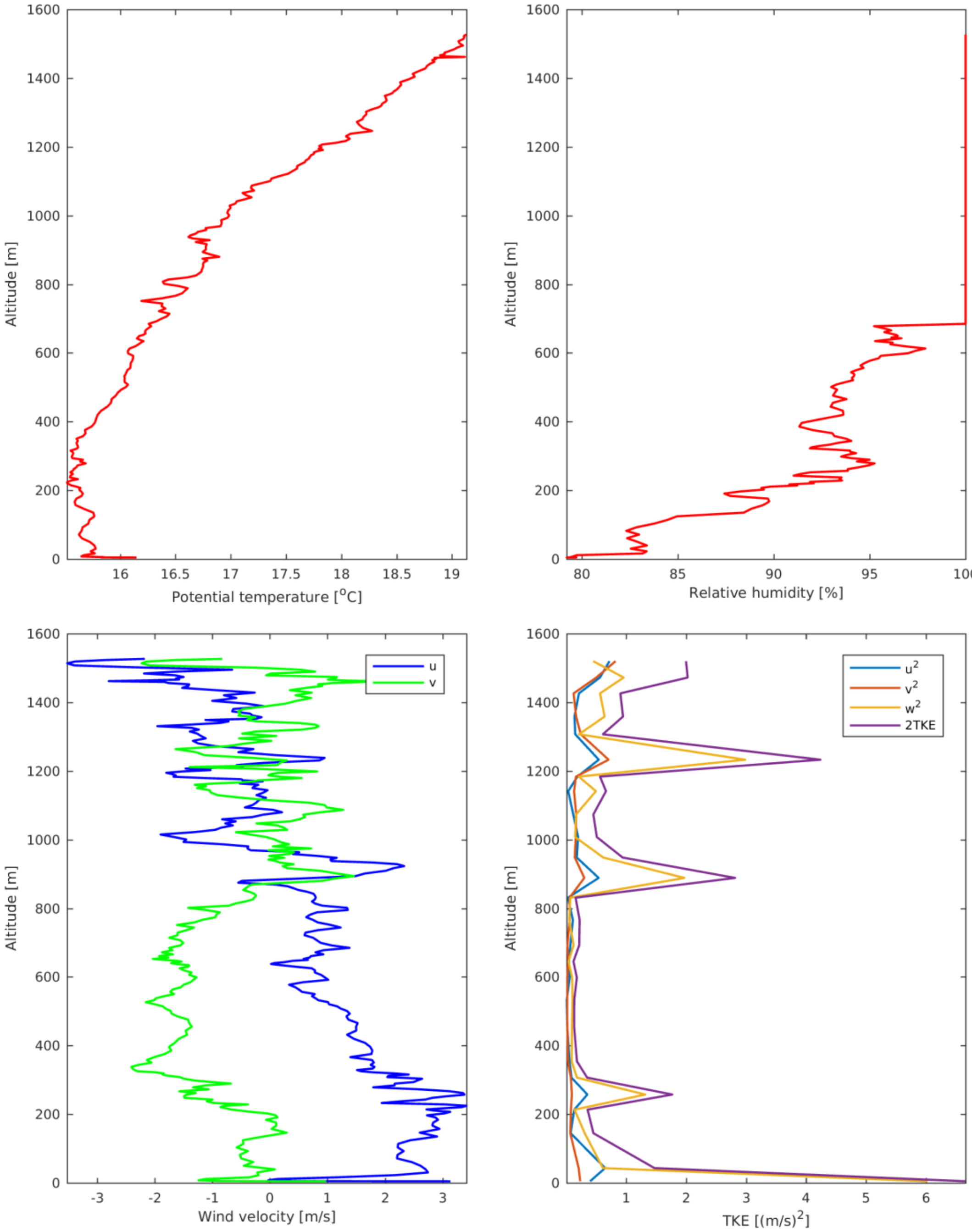

Figure 18. Segment 1 (prof_land1). Vertical profiles of thermodynamic quantities over land during take-off: potential temperature, relative humidity, horizontal wind and TKE.

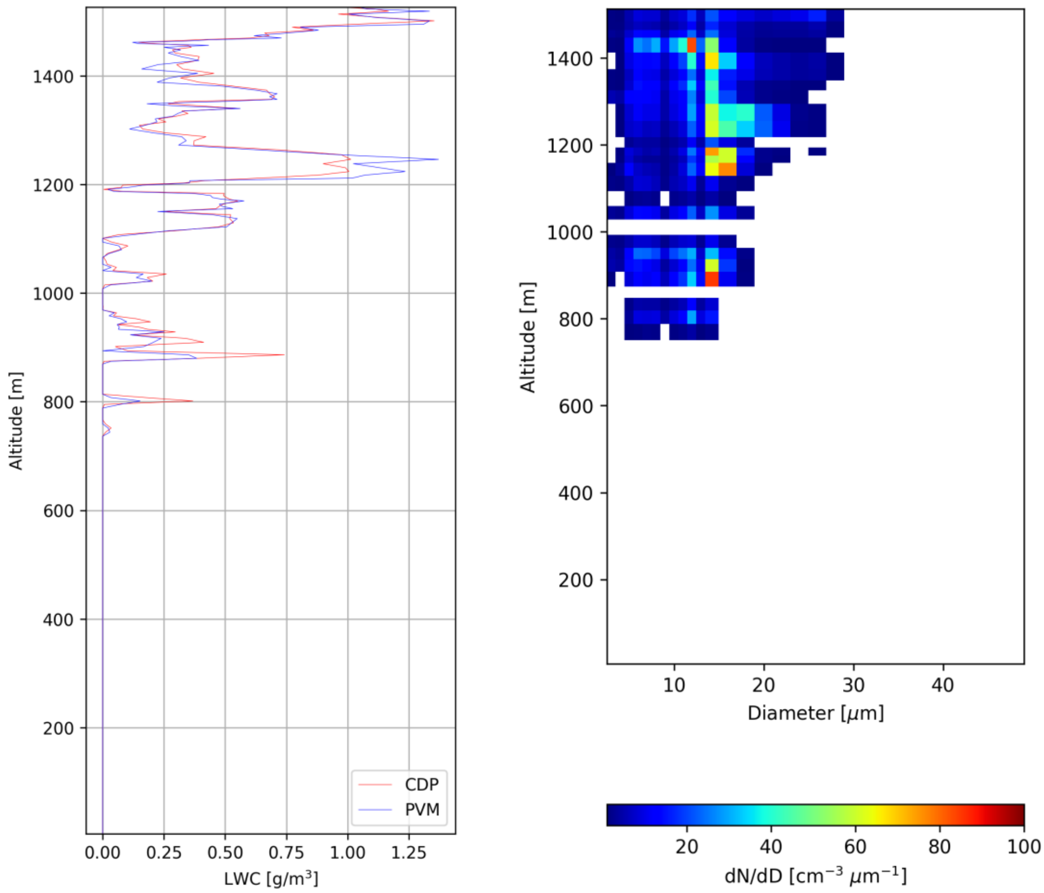

Figure 19. Segment 1 (prof_land1). Cloud microphysics over land during take-off: liquid water content and droplet size distribution versus height.

<u>Landing, segment 24</u>

In the last profile, taken during approaching the airport, one can identify some features similar as described above for the first sounding. Again, there are three main layers, almost at the same heights as before, with different gradients of potential temperature: one neutral and two stable ones. However, an important change has occurred in the 2 hours of flight. Now the lowest layer probably started to mix with the middle one. Horizontal wind does not change significantly between them although fluctuations are much larger in the lower part. TKE value is quite large throughout both of them, up to 900 m, which indicates vigorous daytime convection. It is possible that the middle layer was the residual left from the ABL from the previous day and soon it is going to be well-mixed again with ABL fully developed with its top at ~900 m. At the top, we can observe wind shear, different stability, decrease of TKE and a small cloud. Above, there is the same cloud layer which was identified before. Although the cloud itself resides at slightly different height, the LWC and droplet size distribution is almost perfectly reproduced. Layer decoupling from the surface can be confirmed with wind and TKE profiles.

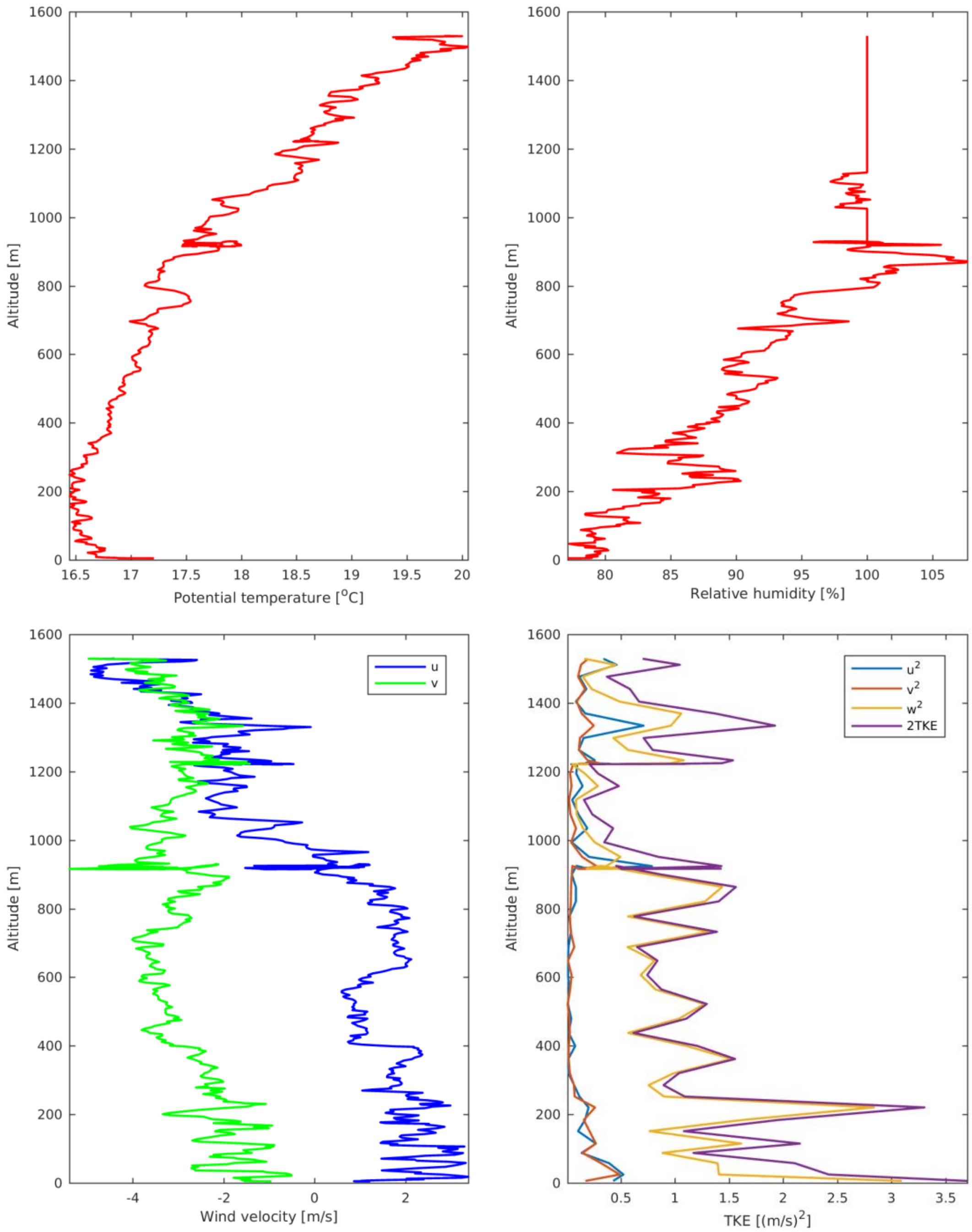

Figure 20. Segment 24 (prof_land2). Vertical profiles of thermodynamic quantities over land during landing: potential temperature, relative humidity, horizontal wind and TKE.

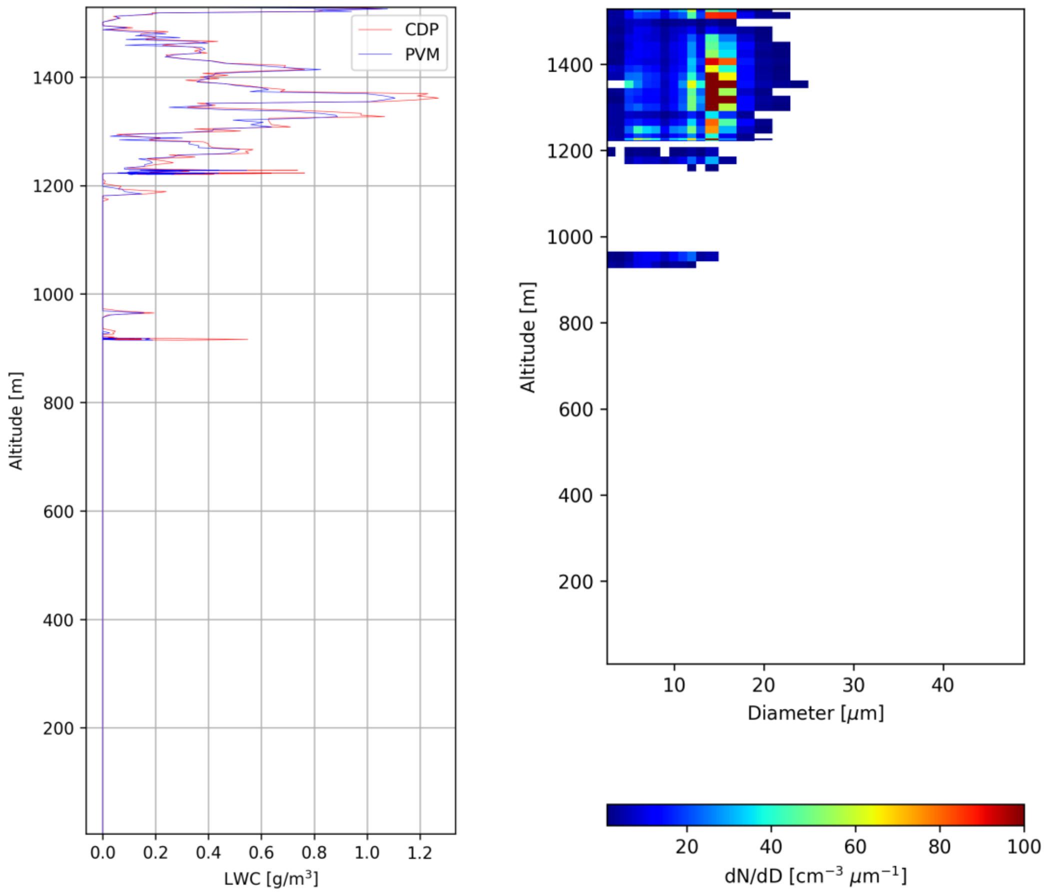

Figure 21. Segment 24 (prof_land2). Cloud microphysics over land during landing: liquid water content and droplet size distribution versus height.

7.1.2. Marine

First descent, segment 5

Over the ocean the vertical structure is even more complicated. First sounding was performed as a straight-line descent starting over Mace Head and heading westward towards open water. The profiles plotted below show many layers differing in their stability (gradient of potential temperature) and dynamics. We have distinguished the following major ones:

1. Well-mixed turbulent surface layer extending from the ground up to ~ 150 m. Constant potential temperature is the sign of neutral stability. Horizontal wind fluctuates with height which agrees with moderate, but clearly higher than for other layers, values of turbulent kinetic energy. Turbulence in such a low-level layer is generated by friction or by weak convection. Unfortunately, for obvious reasons the profile could not have been completed down to the water surface. The air mass inside is pretty humid, which is easily understandable, because ocean is great source of moisture. At its top, the layer is capped with temperature inversion accompanied with a drop in humidity. Thus, the mixing with the upper part of the atmosphere is rather limited.
2. From 150 m up to 300 m, containing linear profiles of temperature, wind and humidity. It might be a residual layer left from the boundary layer developed during past days.
3. From 300 m up to 500 m, another intermediate layer with parameters changing with height. It seems to have a non-trivial vertical structure itself. Interestingly, there is some little turbulence inside.

4. From 500 m up to 900 m, analogous to the former one.
5. The cloud layer extending from 900 m upwards with cloud base approx. at 1100 m. The cloud contains moderate liquid water content. LWC increases almost linearly with height which suggest a horizontally homogeneous cloud layer.

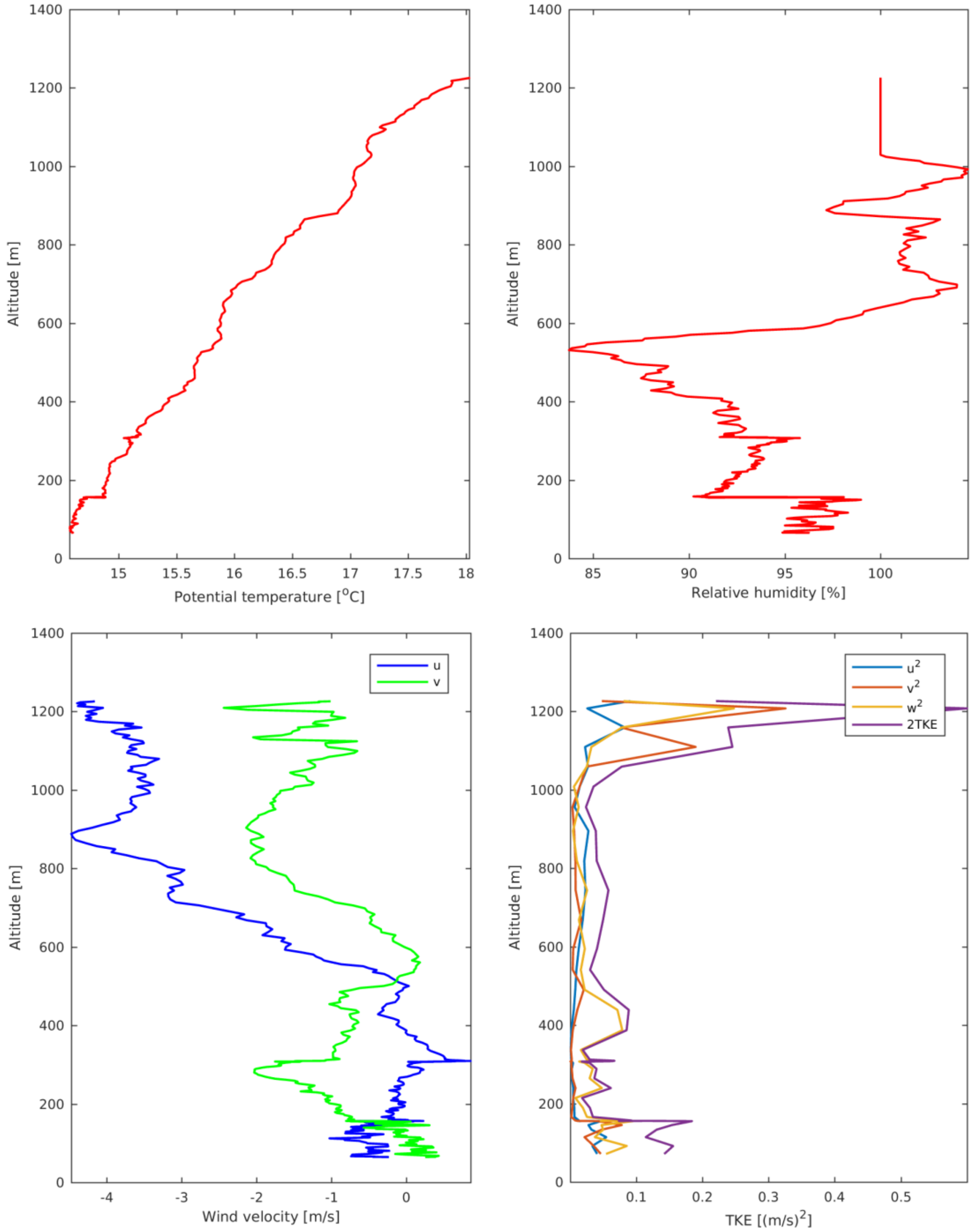

Figure 22. Segment 5 (prof_oce1). Vertical profiles of thermodynamic quantities over land during landing: potential temperature, relative humidity, horizontal wind and TKE.

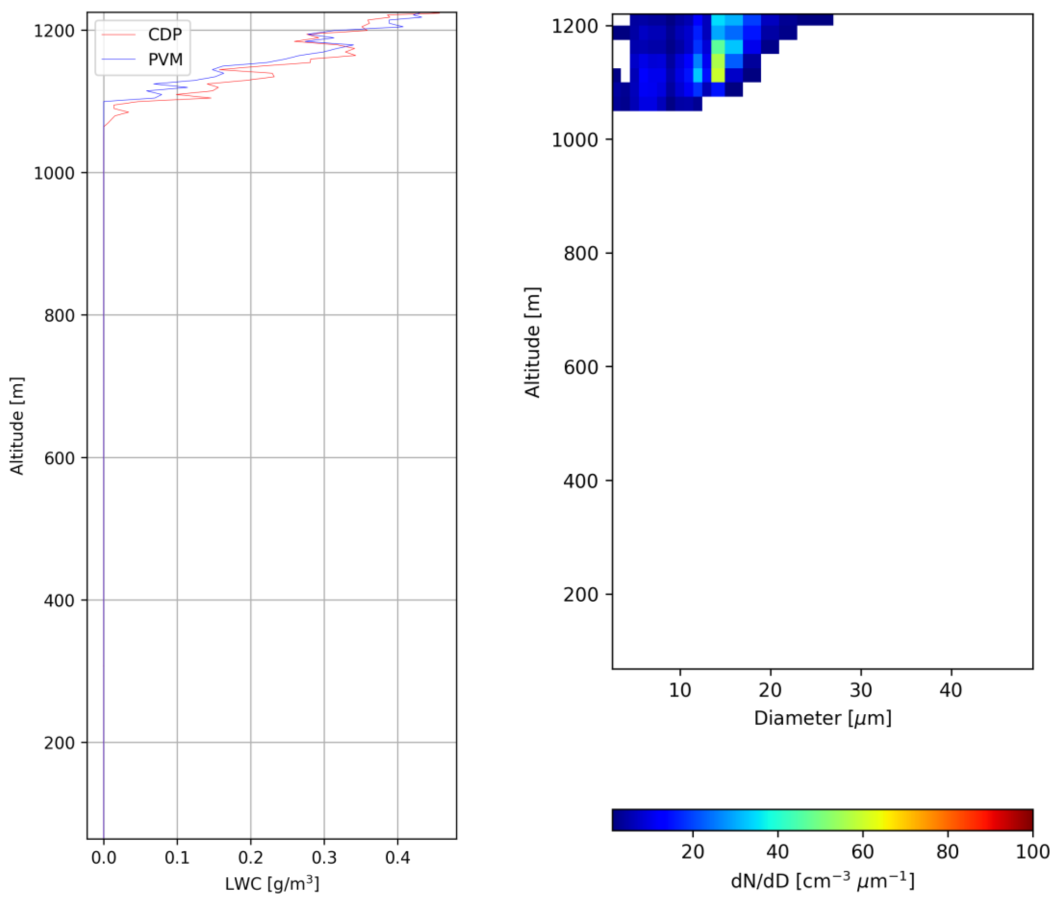

Figure 23. Segment 5 (prof_oce1). Cloud microphysics over land during landing: liquid water content and droplet size distribution versus height.

<u>Last descent, segment 20</u>

The second sounding over ocean was performed as straight-line descent on the way from waypoint F towards Shannon airport, so the actual location in space is not the same as for the former described above. Nevertheless it was also completed safely over ocean. Worth to mention, the aircraft sampled the atmosphere almost at the same time as the balloon sounding was made at the station Valentia (12 UTC) and one can spot striking qualitative correspondence. Following features are easy to identify:

1. Well-mixed, turbulent boundary layer extending up to 400 m and capped with a shallow cloud under temperature inversion. It is possible that the layers (1) and (2) from the previous sounding, i.e. morning developing boundary layer and residual layer, have been mixed, lifting temperature inversion up to 400 m. Because both of them were abundant in moisture, it was easy to start condensation and built cloud at the top.
2. The layer between 400 and 1100 m, might correspond with (3), (4) and (5) from last sounding. They seem to have been squeezed a bit and are capped with strong temperature inversion accompanied by sharp drop in humidity. The inversion and squeezing might be connected with subsidence in the higher pressure advancing from the west (compare surface analysis in figure 6). There is no cloud at this level but such observation is explained by different place of the profile. Looking again at satellite image with flight trajectory (figure 9), one would see that higher, deeper clouds occupy mostly the land and reach a few kilometers to the west into the ocean.

However, further over the water, there are only lower shallow stratiform clouds. Exactly such cloud was penetrated.

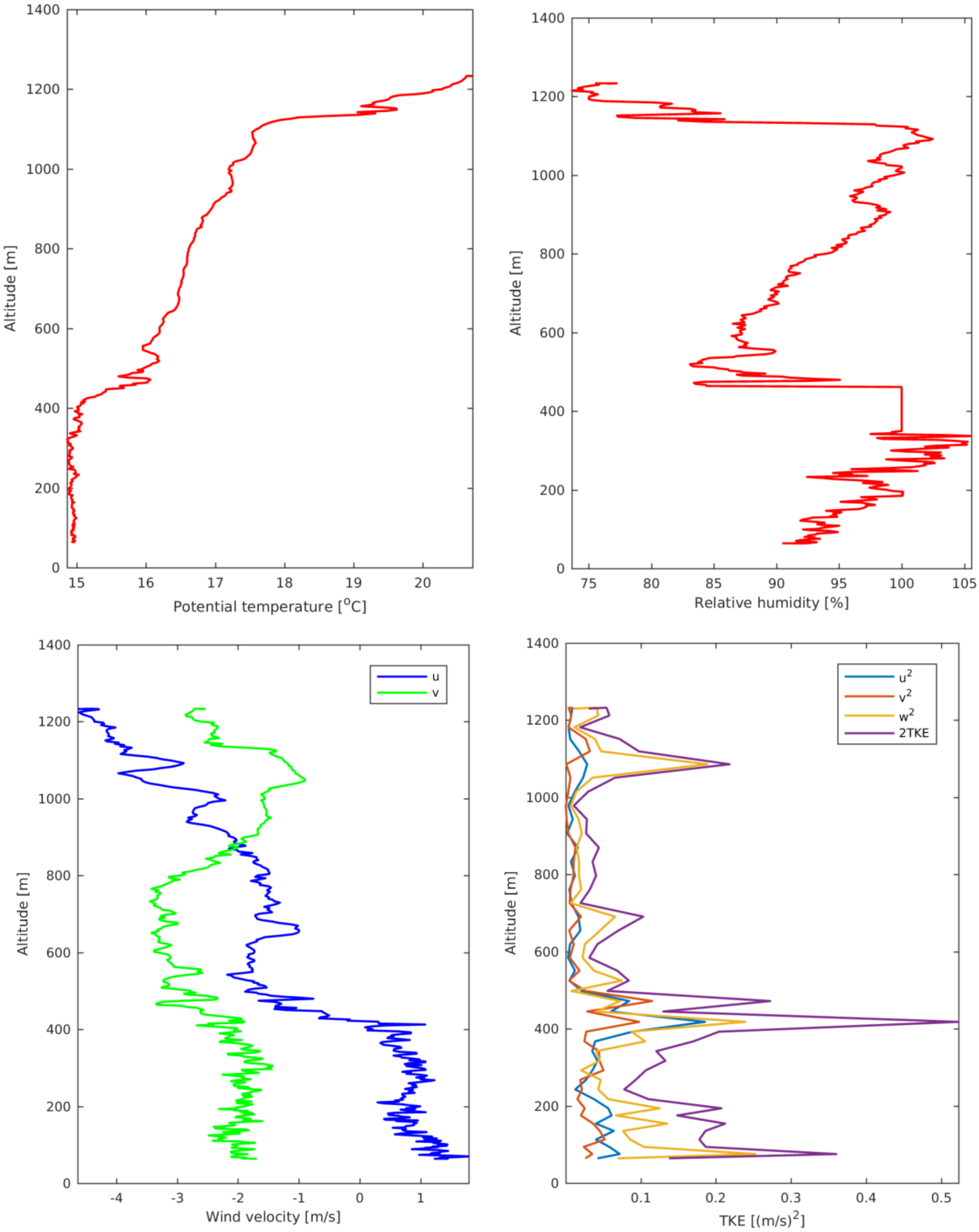

Figure 24. Segment 20 (prof_oce2). Vertical profiles of thermodynamic quantities over land during landing: potential temperature, relative humidity, horizontal wind and TKE.

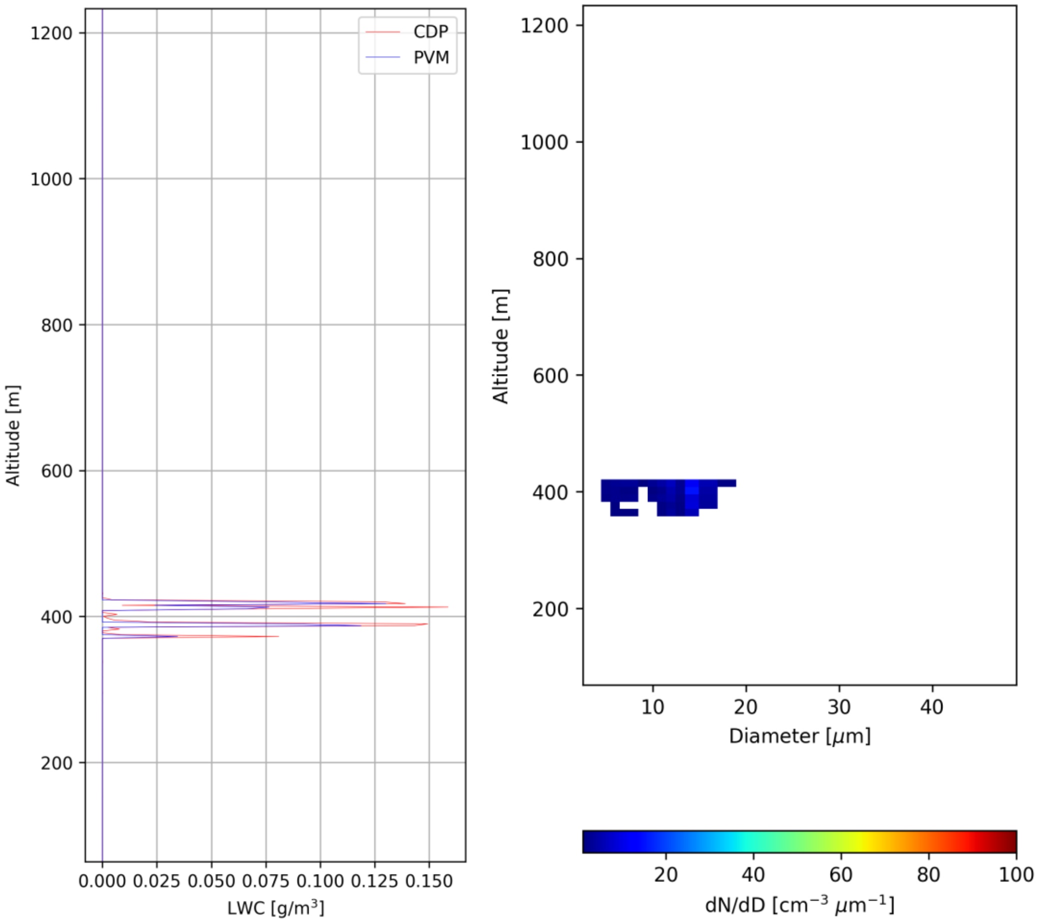

Figure 25. Segment 20 (prof_oce2). Cloud microphysics over land during landing: liquid water content and droplet size distribution versus height.

7.2. HORIZONTAL VARIABILITY IN THE ATMOSPHERE

In this section we study transitions between adjacent horizontal legs flown over land and over ocean at different heights in terms of dynamics, thermodynamics and cloud microphysics. We start with the lowest level and go upwards. Unfortunately, due to local topography, visibility conditions and resulting safety regulation the lowest land leg was done only at ~405 m (above sea level). The table below gives overview of the mean conditions for each of the horizontal segments. It contains average values of temperature, potential temperature, relative humidity, absolute humidity, components of wind velocity, turbulent kinetic energy and liquid water content.

Table 4. Average conditions for horizontal legs.

Seg.	Leg ID	Height [m]	T [C]	Tpot [C]	RH [%]	a [g/m3]	u [m/s]	v [m/s]	w [m/s]	TKE [m2/s2]	LWC [g/m3]
6	oce1	64	14.0	14.5	97	11.7	0.0	-0.6	0.2	0.05	0.01
21	oce6	65	14.4	14.9	92	11.3	2.1	-2.3	0.2	0.13	0.00
8	oce2	163	13.2	14.6	98	11.3	1.3	-1.3	0.2	0.06	0.01
10	mix1	279	13.0	15.6	90	10.3	1.6	0.0	0.2	0.29	0.01

12	land3	404	12.3	16.1	93	10.1	0.3	-1.1	0.2	0.29	0.00
13	oce3	406	11.8	15.5	92	9.6	-0.1	-1.7	0.2	0.05	0.01
16	land4	741	9.7	16.8	100	9.2	-0.4	-2.6	0.1	0.16	0.02
15	oce4	741	9.4	16.5	96	8.7	-1.0	-1.9	0.1	0.05	0.00
4	land2	1225	6.8	18.6	100	7.6	-3.1	0.0	0.1	0.27	0.36
18	land5	1230	7.3	19.2	98	7.7	-3.2	-2.1	0.1	0.08	0.15
19	oce5	1231	7.4	19.3	94	7.4	-4.9	-1.2	0.1	0.08	0.15
2	land1	1529	4.7	19.6	101	6.8	-3.1	0.4	0.1	0.24	0.45
23	mix2	1531	5.1	20.0	100	6.9	-4.9	-2.1	0.4	0.23	0.11

7.2.1 First level, ~ 65 m

At the lowest level, two legs were performed over ocean, one at the beginning of the flight and another close to the end. The height was dictated by safety regulations. Both segments are relatively short (3 min), so calculating surface fluxes would encounter serious difficulties. However, one can look how the conditions have changed in the course of around 1.5 hour. Temperature and relative humidity stayed almost the same. The latter is close to saturation, because ocean surface is an efficient source of moisture.
Horizontal wind has significantly increased which is also reflected in turbulent kinetic energy, presumably produced by surface friction. Measured wind velocity corresponds well with vertical soundings. Interestingly, wind profile seems to be homogenized during the flight - at the time of the second leg it takes the value earlier present at around 300 m. This facts confirms the hypothesis of growing boundary layer. The air mass below 400 m has been mixed and vertical momentum from its upper part transported towards the surface.
No clouds were observed at 65 m above sea level. Otherwise the aircraft would not be able to fly so close to the surface.

<u>Marine, segment 6 (leg_oce1)</u>

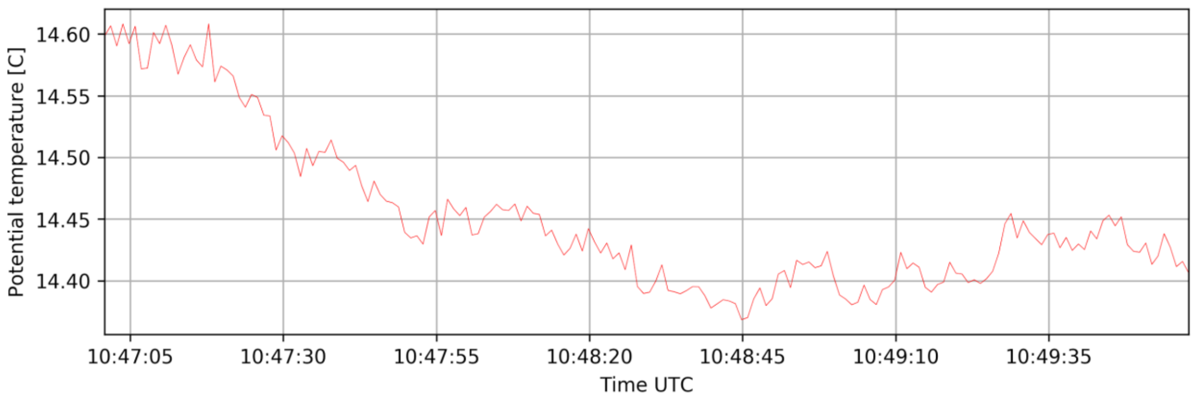

Figure 26.a. Segment 6. Potential temperature.

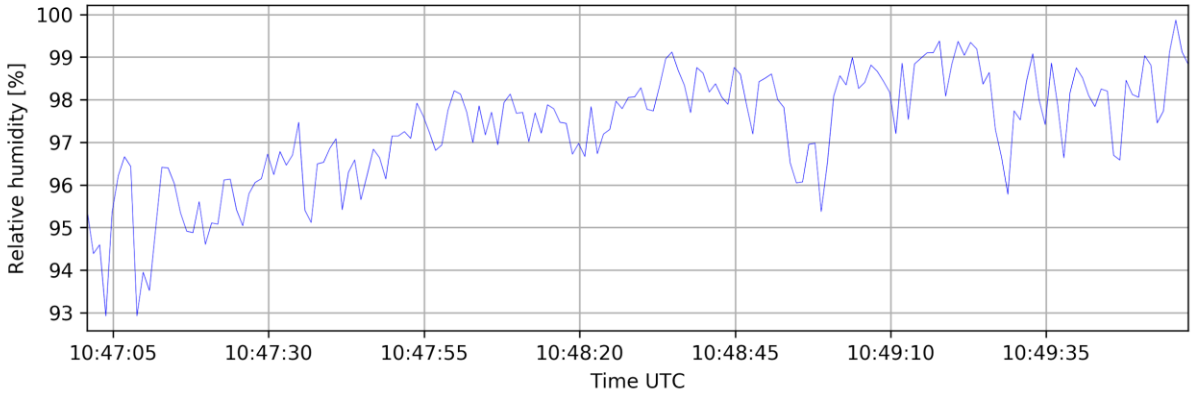

Figure 26.b. Segment 6. Relative humidity.

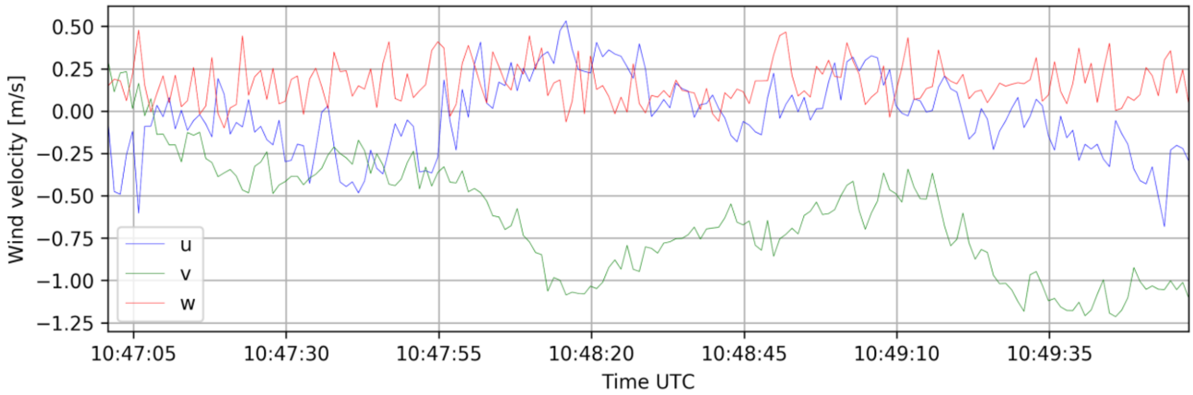

Figure 26.c. Segment 6. Wind velocity components.

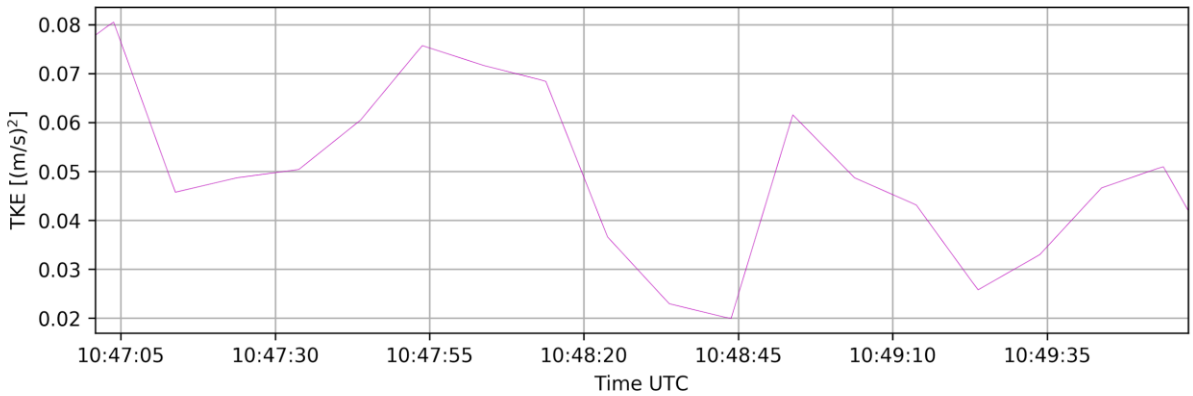

Figure 26.d. Segment 6. Turbulence kinetic energy.

<u>Marine, segment 21 (leg_oce6)</u>

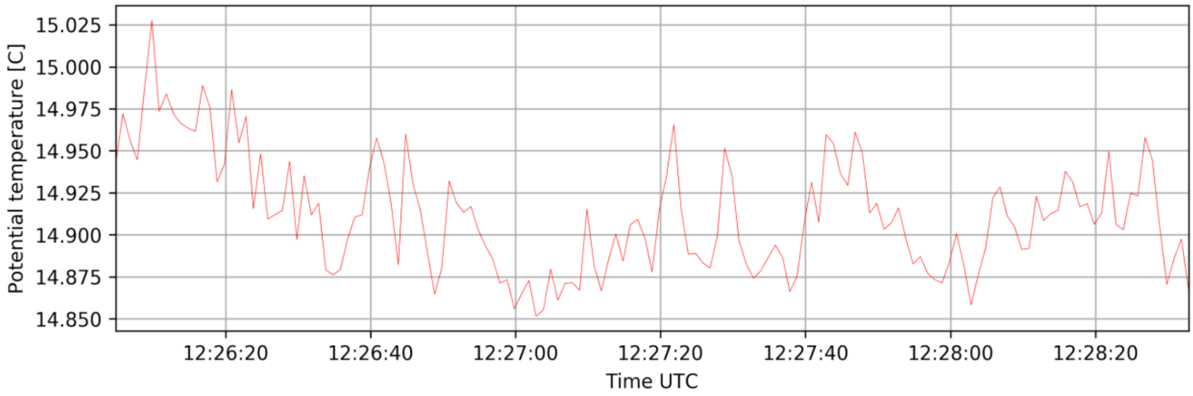

Figure 27.a. Segment 21. Potential temperature

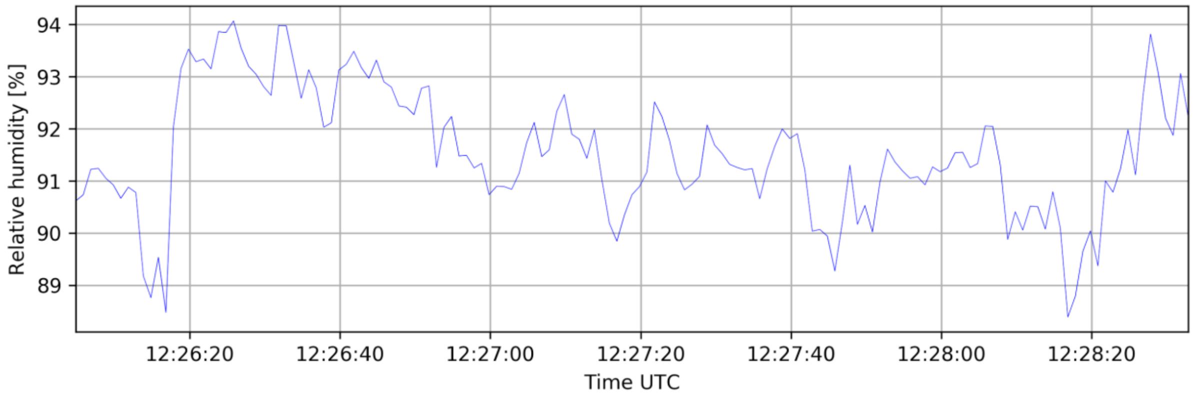

Figure 27.b. Segment 21. Relative humidity.

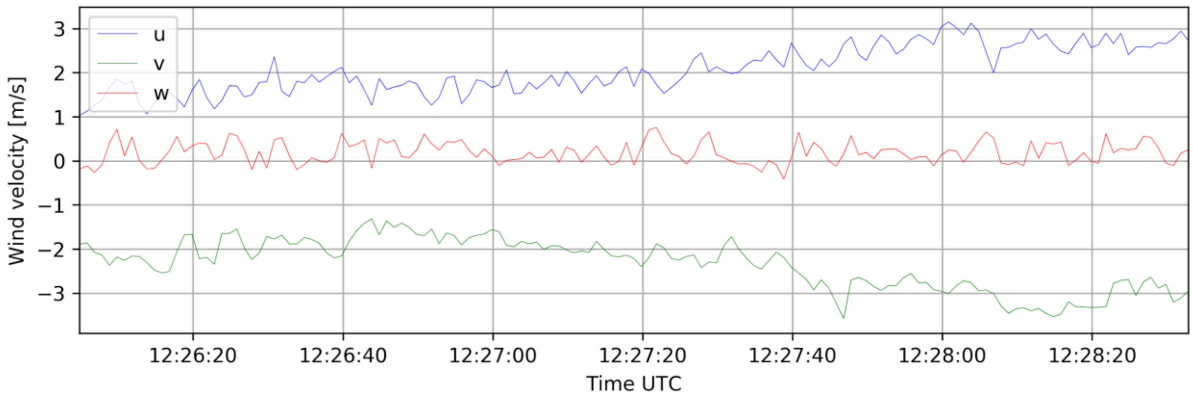

Figure 27.c. Segment 21. Wind velocity components.

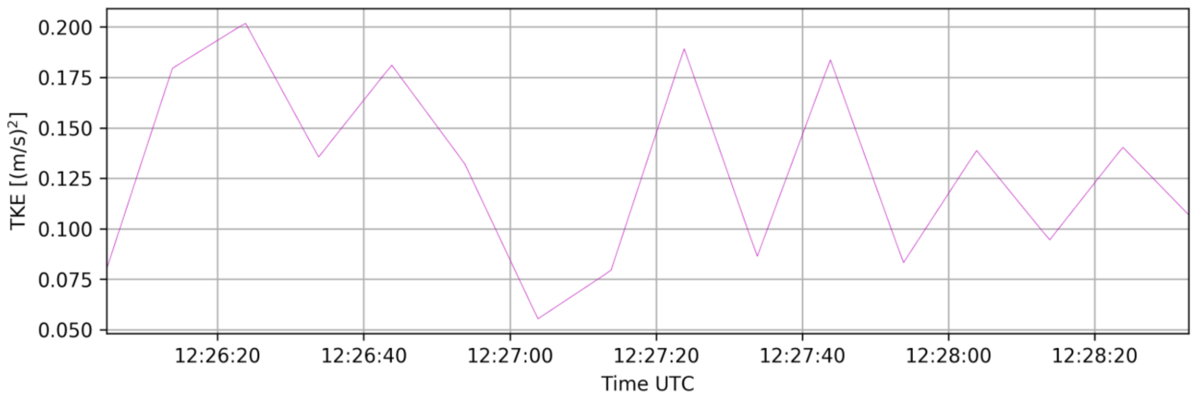

Figure 27.d. Segment 21. Turbulence kinetic energy.

7.2.2 Second level, ~ 165 m

The second level is located close to the top of the well-mixed layer from the first sounding over ocean. The values of potential temperature and relative humidity are similar to the previous layer. There is probably dynamic contact between them. The record of horizontal wind initially shows the change to the speed and direction characteristic for the level 300 m in the first profile and the whole bottom layer in the second profile (u=1 m/s, v=-2 m/s). Then there is a patch of increased turbulence, which compares well with the local maximum in TKE in the first sounding. Finally, when approaching the shore, horizontal winds turns its direction. The facts mentioned here suggest that the features observed in the soundings which we assigned to the boundary layer evolution, might be as well remnants of horizontal inhomogeneity. Indeed, the soundings were flown as straight line descents, in contrast to vertical spirals often performed in airborne experiments.

Marine, segment 8 (leg_oce2)

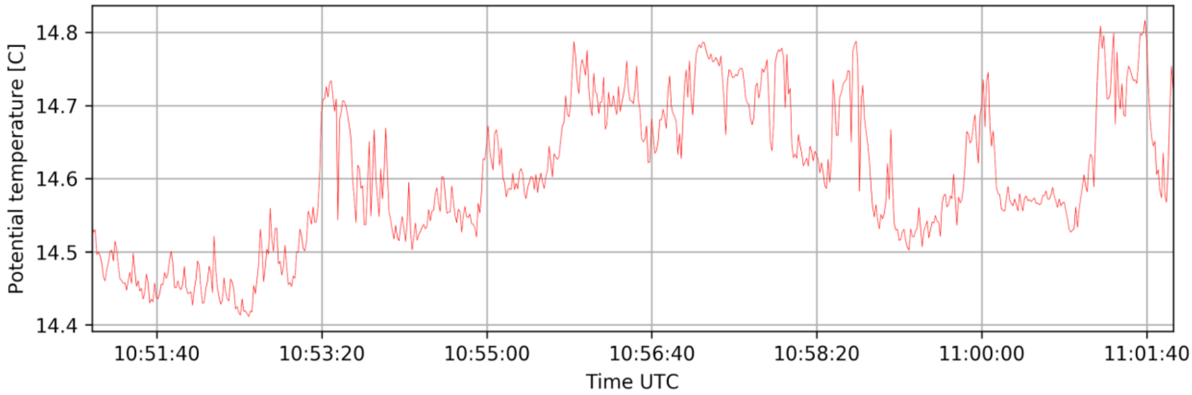

Figure 28.a. Segment 8. Potential temperature.

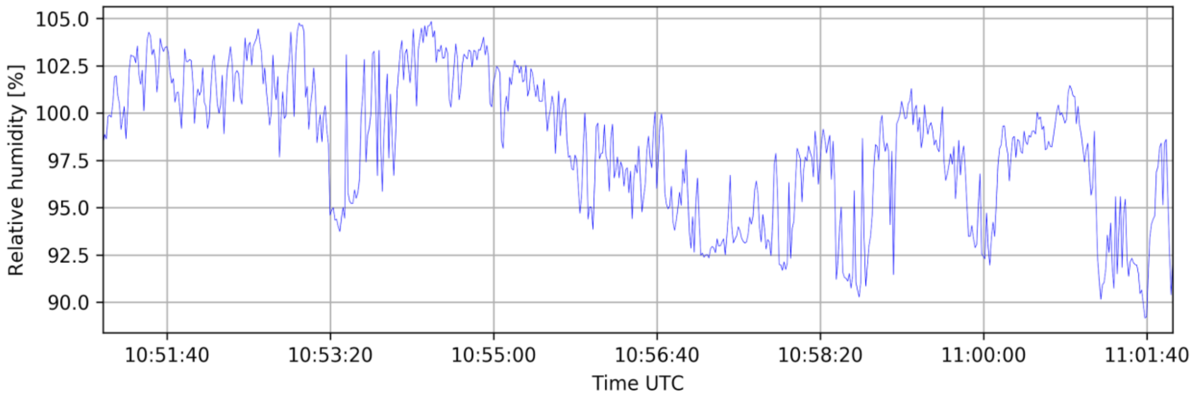

Figure 28.b. Segment 8. Relative humidity.

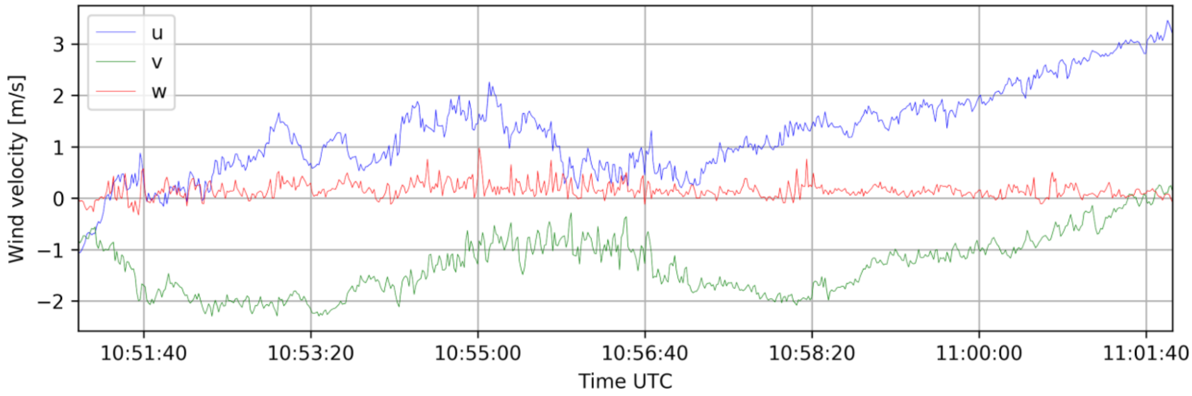

Figure 28.c. Segment 8. Wind velocity components.

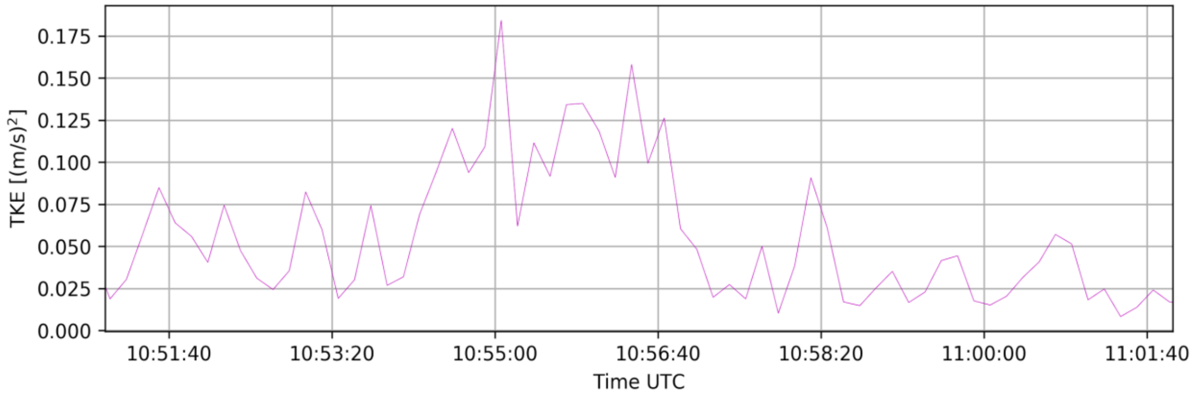

Figure 28.d. Segment 8. Turbulence kinetic energy.

7.2.3 Third level, ~ 405 m

In a sense, three legs were done at the third level because the one over land was twice as long as usual and included a turn in the middle. Thus, one can look whether patterns recorded in the first half of the segments are reproduced in the reversed order in the second half. Indeed, in the plots below one can find a slight drop in temperature at the beginning of the continental leg accompanied by an increase in zonal wind component and followed by a significant drop in humidity. On the way back, this pattern is reversed. The depletion of humidity goes first, before a drop in temperature and higher wind velocity. In the mentioned moments the aircraft is close to the seashore and the wind is blowing eastward, i.e. from the ocean towards land, with the speed of ~2 m/s. We may speculate whether it is a sign of local sea breeze circulation. Even so, it is not very plausible to measure it at such altitude. In the middle of the leg there is another decrease in humidity and local maximum of temperature. In general temperature fluctuations are anti-correlated with those in humidity. This might result from mixing with warmer drier air from above.

In the signals recorded during the flight over ocean, there are several penetrations of small clouds. Non-zero liquid water content coincides with saturation, jumps in temperature as well as increased variability of wind velocity and higher TKE. It is the same cloud layer as penetrated in the second sounding over ocean, visible also in the satellite image. There is also evident drop in temperature after passing the second patch of clouds. Recalling the profile, we suppose it is crossing of the 1 K inversion capping the cloud and bottom part of the atmosphere which we expect to be a boundary layer.

The transition between continental and marine part of the flight is not sharp. However, we observe striking difference in wind fluctuations and turbulent kinetic energy. Obviously, they are connected with each other and significantly higher over land. It is caused either by daytime convection induced by solar radiation heating the land surface much more efficiently than the water or by the more vigorous friction generated mixing due to much higher roughness of the land surface.

Continental, segment 12 (leg_land3)

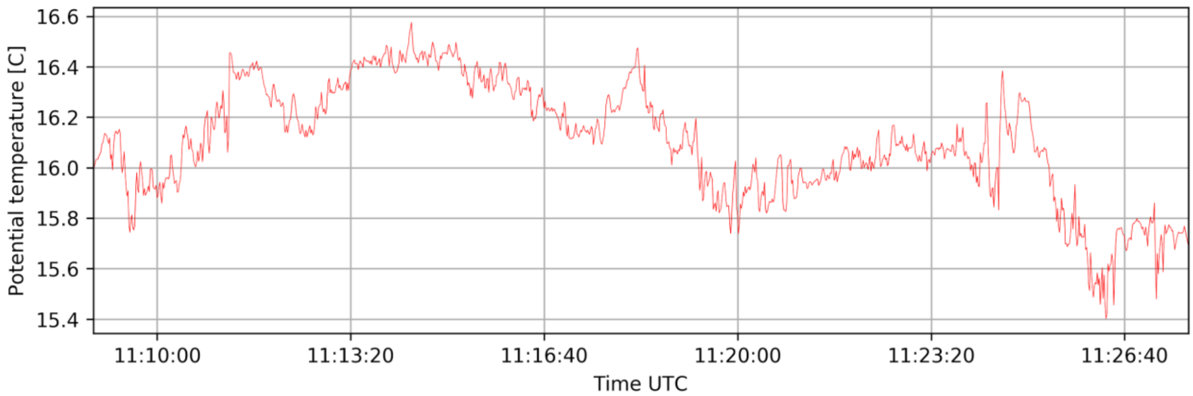

Figure 29.a. Segment 12. Potential temperature.

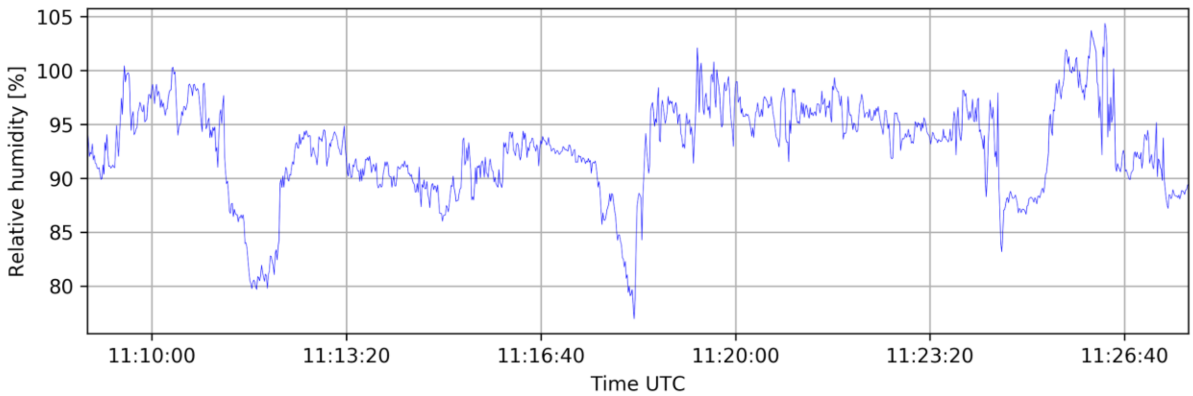

Figure 29.b. Segment 12. Relative humidity.

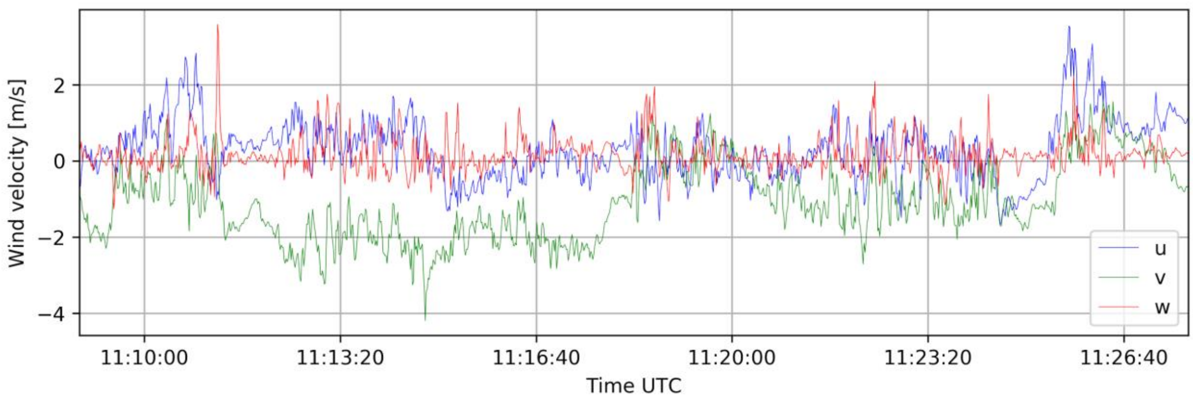

Figure 29.c. Segment 12. Wind velocity components.

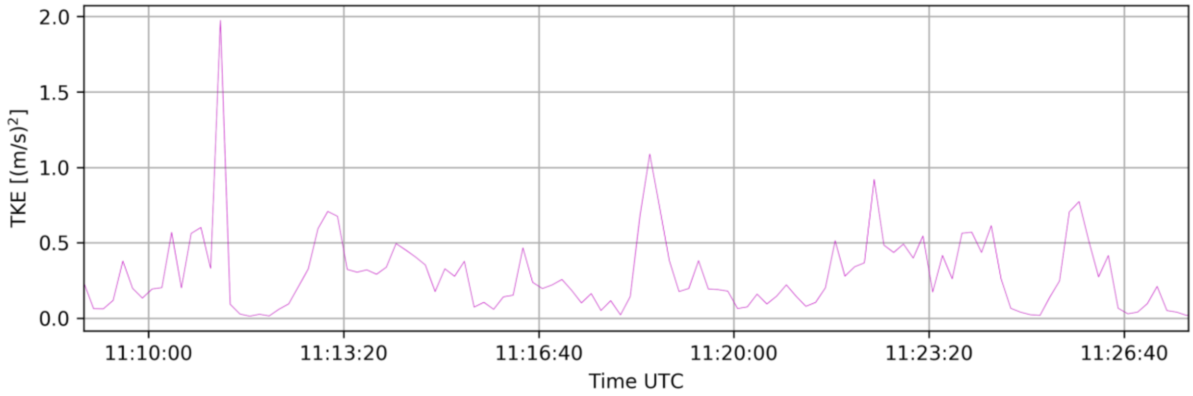

Figure 29.d. Segment 12. Turbulent kinetic energy.

<u>Marine, segment 13 (leg_oce3)</u>

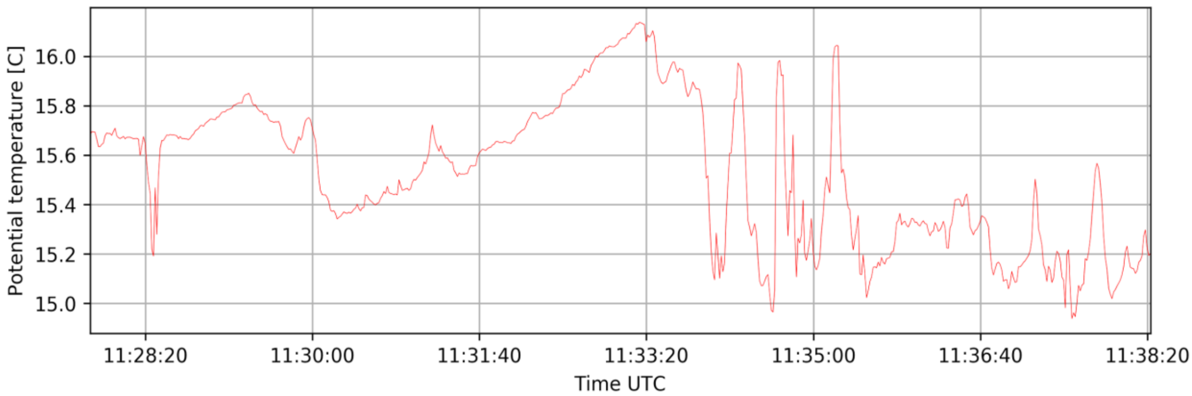

Figure 30.a. Segment 13. Potential temperature.

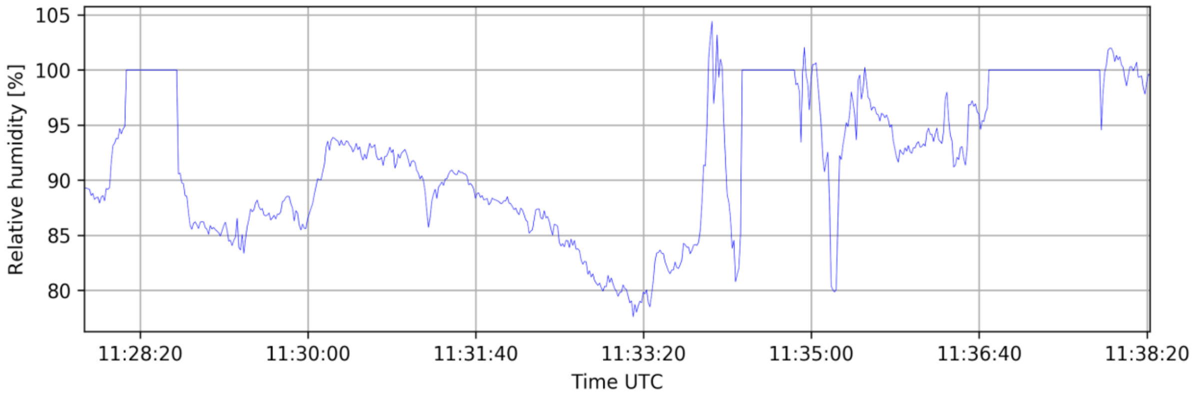

Figure 30.b. Segment 13. Relative humidity.

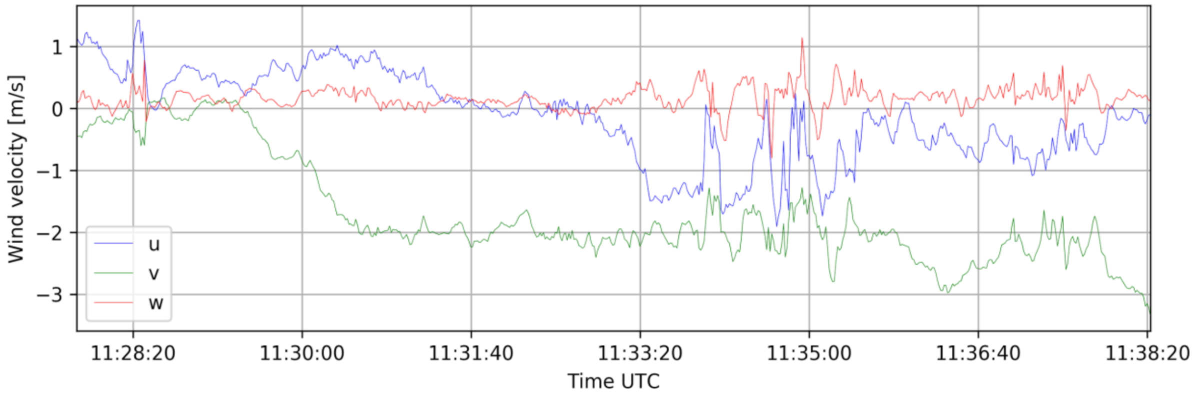

Figure 30.c. Segment 13. Wind velocity components.

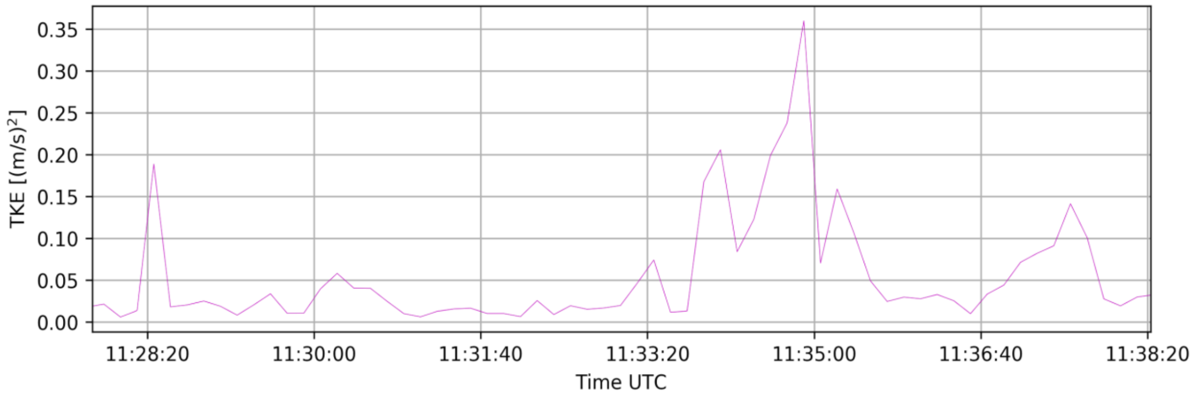

Figure 30.d. Segment 13. Turbulent kinetic energy.

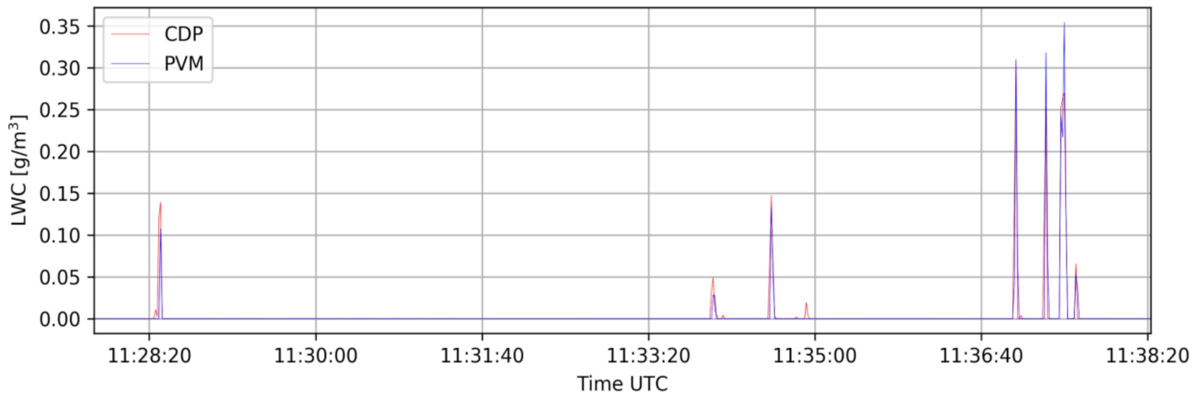

Figure 30.e. Segment 13. Liquid water content.

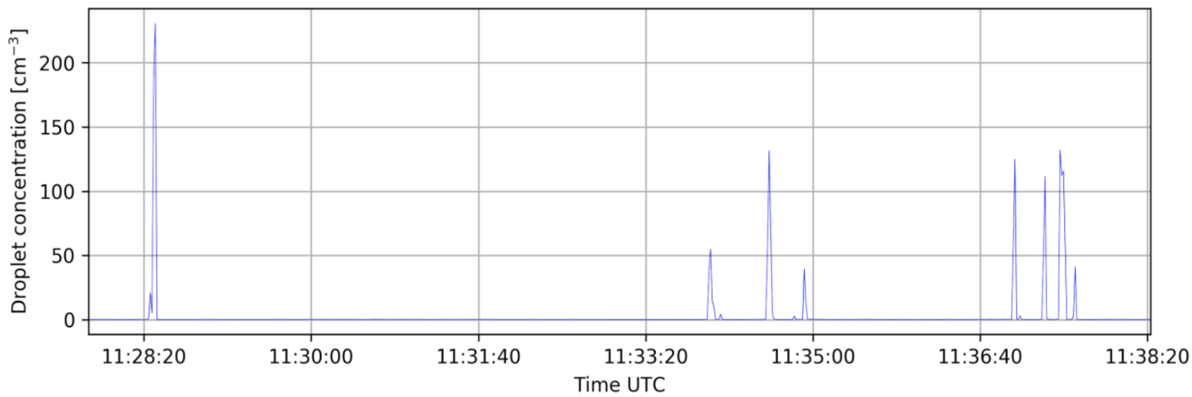

Figure 30.f. Segment 13. Cloud droplet number concentration.

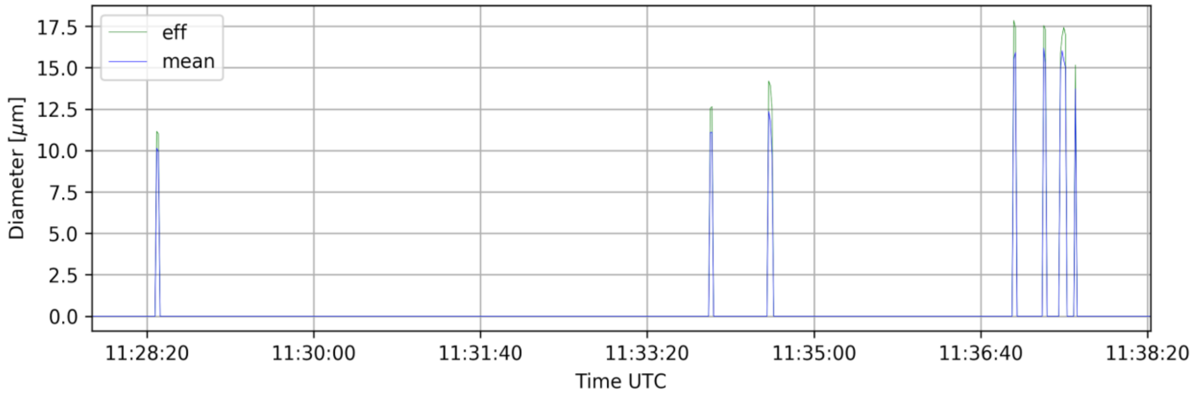

Figure 30.g. Segment 13. Mean and effective droplet diameter.

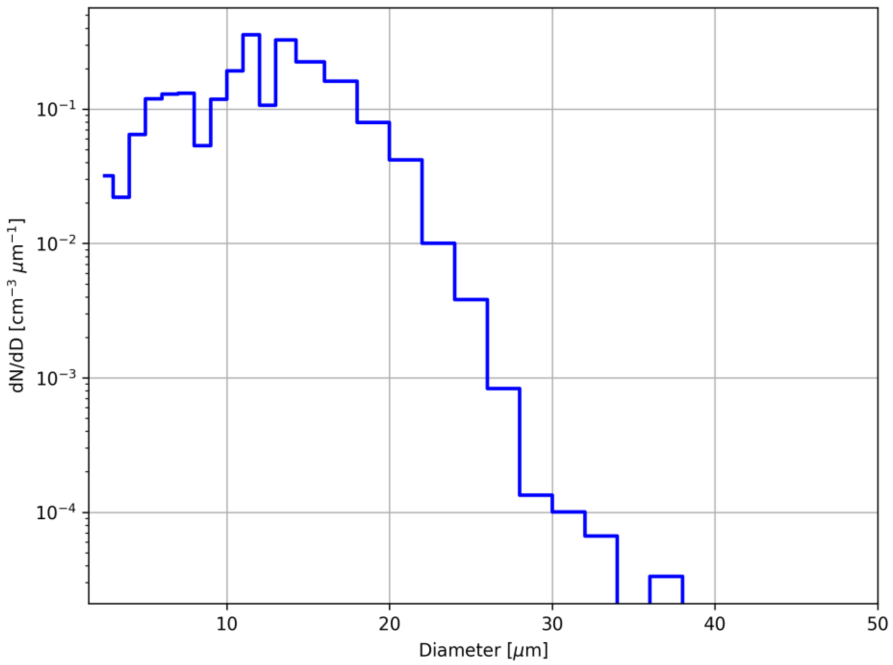

Figure 30.h. Segment 13. Droplet size distribution integrated over the leg.

7.2.4 Fourth level, ~ 740 m

At the altitude of 740 m the difference between marine and continental part of the leg is not very clear. Definitely, there is more dynamic mixing in the latter, visible in fluctuations in temperature, humidity and wind velocity. It starts even at the end of the ocean leg. However, this observation can be as well assigned to the presence of clouds. Liquid water content values are a bit higher than in the previous level over ocean. It is mainly due to higher droplet concentration while mean and effective droplet diameters are rather smaller although they resides at considerably larger height. The clouds might have originated in a more polluted environment. Indeed, droplet number concentration grows while flying further into the island. At the same time mean droplet sizes decrease. Yet, we cannot be completely sure whether all three cloud patches had the same past evolution. Relative humidity repeatedly takes values higher than 100 % corresponding to saturation. It is presumably an instrumental artifact rather than real supersaturation which is known to rarely exceed fraction of a percent.

Marine, segment 15 (leg_oce4)

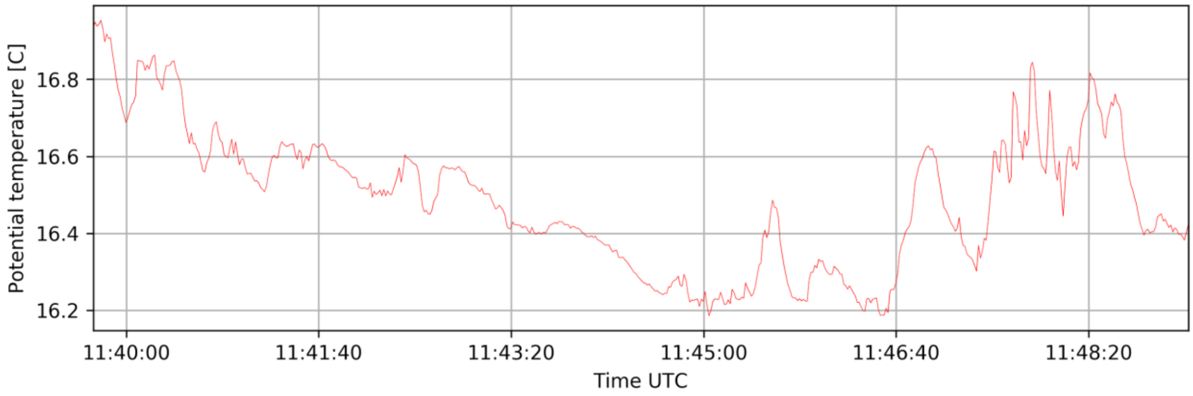

Figure 31.a. Segment 15. Potential temperature.

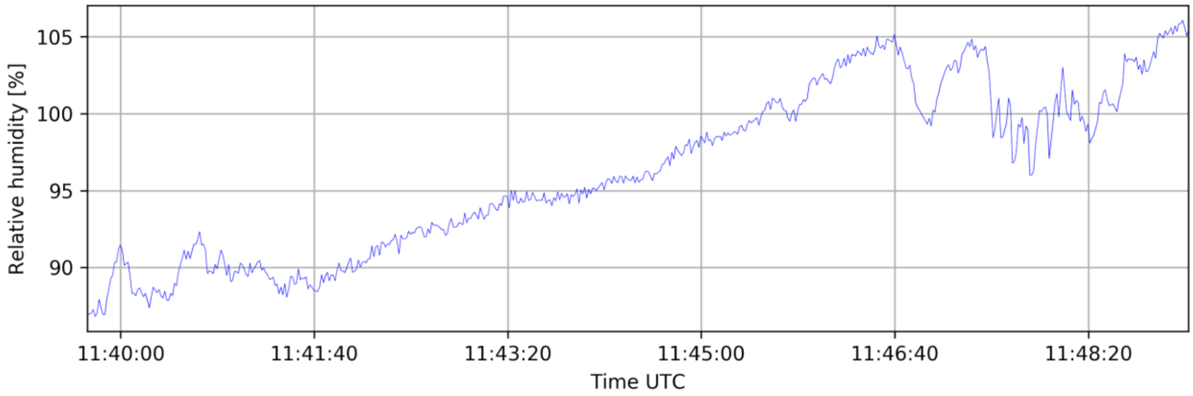

Figure 31.b. Segment 15. Relative humidity.

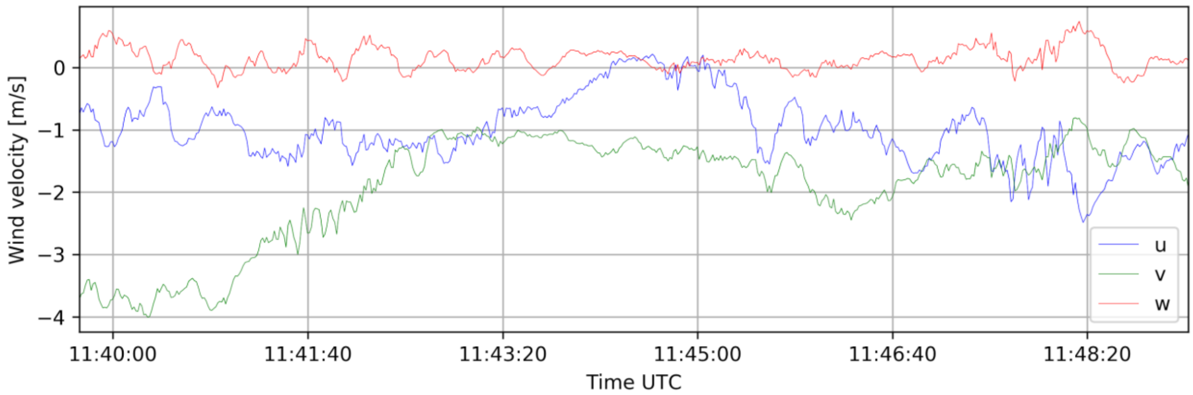

Figure 31.c. Segment 15. Wind velocity components.

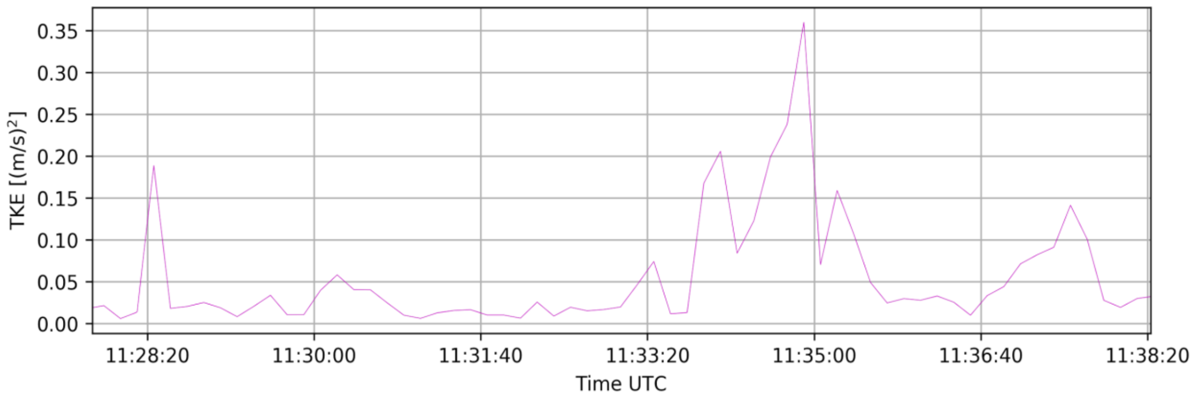

Figure 31.d. Segment 15. Turbulence kinetic energy.

Continental, segment 16 (leg_land4)

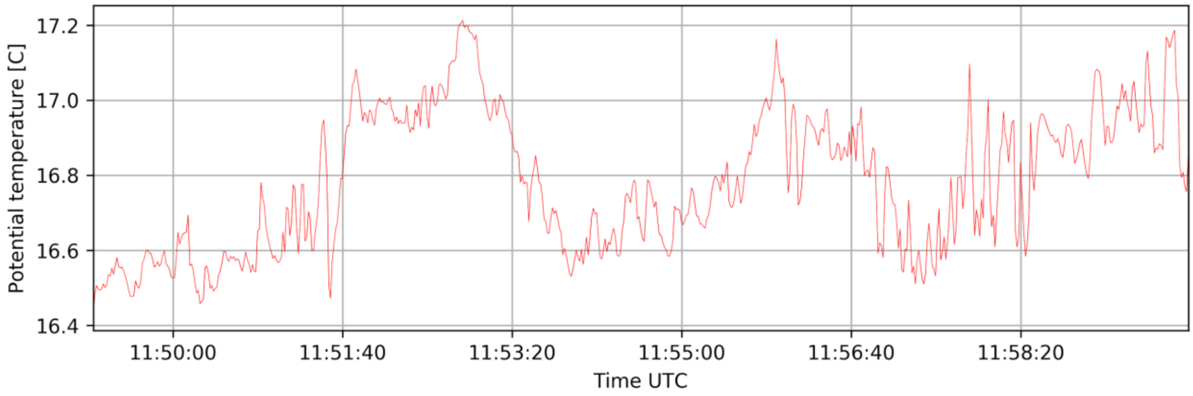

Figure 32.a. Segment 16. Potential temperature.

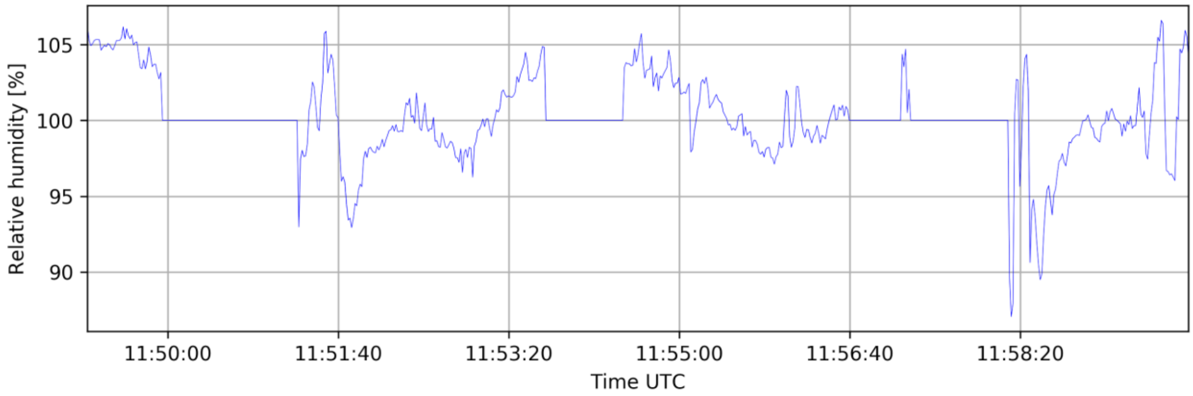

Figure 32.b. Segment 16. Relative humidity.

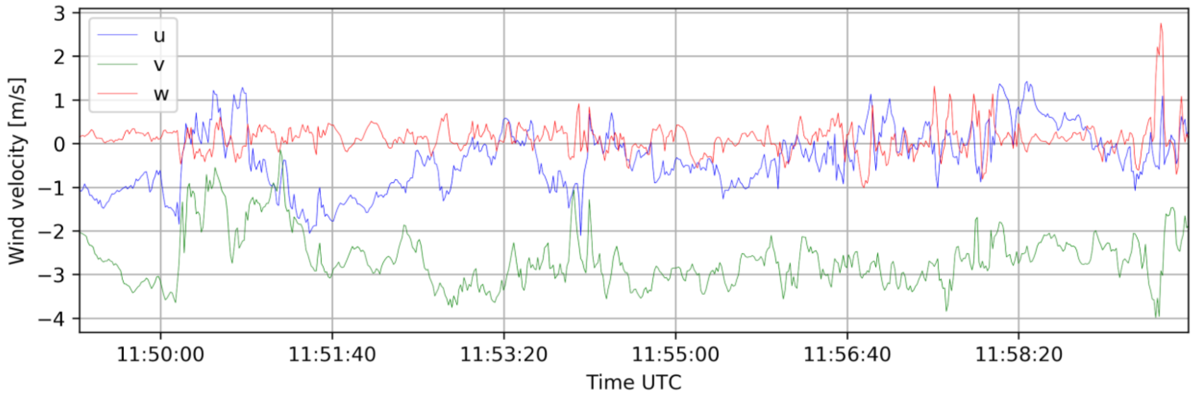

Figure 32.c. Segment 16. Wind velocity components.

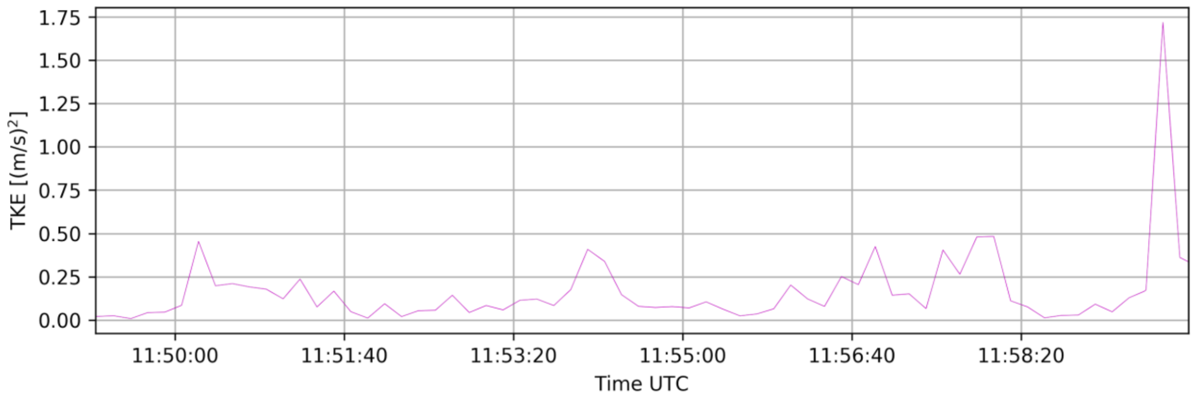

Figure 32.d. Segment 16. Turbulence kinetic energy.

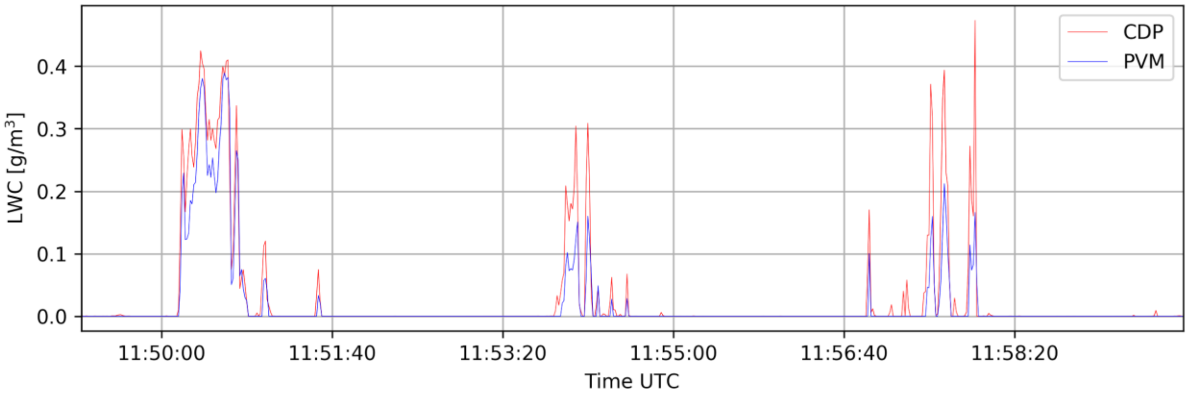

Figure 32.e. Segment 16. Liquid water content.

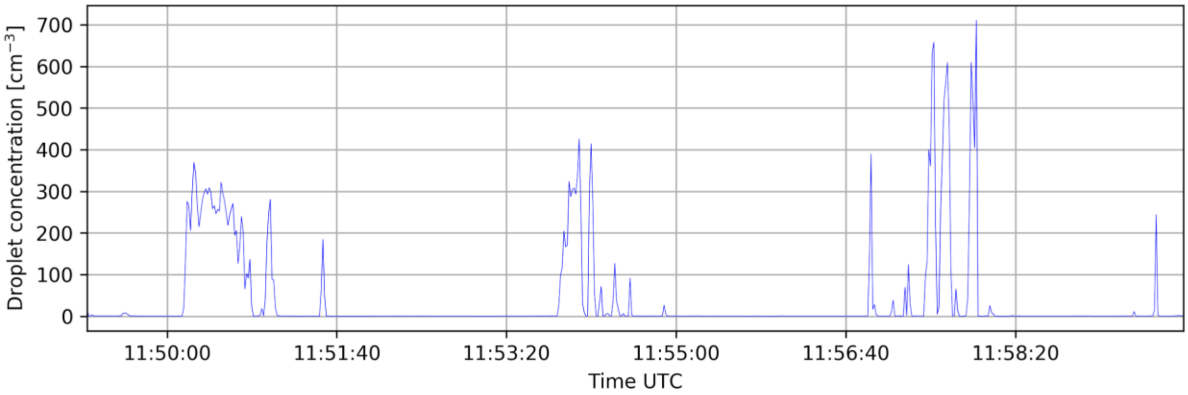

Figure 32.f. Segment 16. Cloud droplet number concentration.

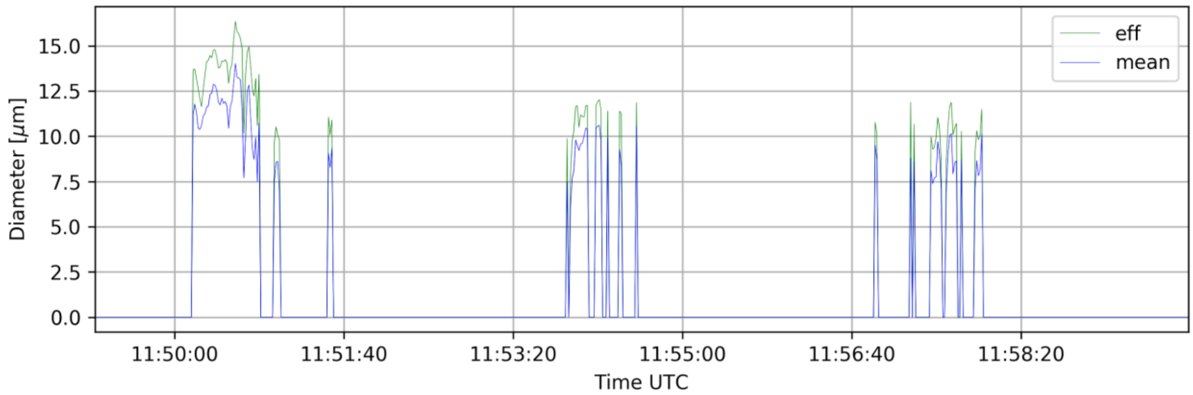

Figure 32.g. Segment 16. Mean and effective droplet diameter.

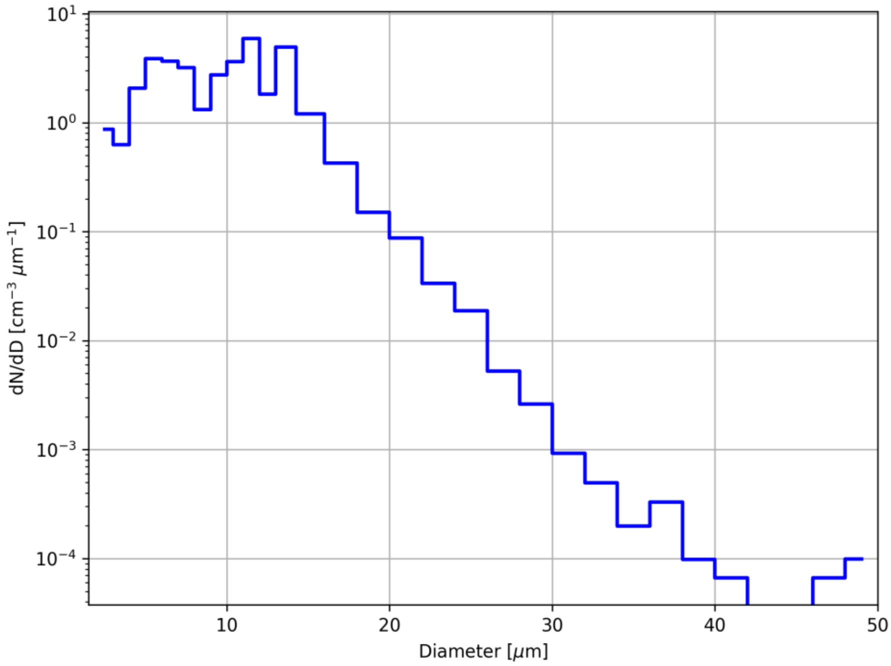

Figure 32.h. Segment 16. Droplet size distribution integrated over the leg.

7.2.5 Fifth level, ~ 1230 m

At the highest altitude of 1230 m, in total three horizontal legs were performed. First was done over the land at the beginning of the flight, shortly before first descent towards the ocean. Another two, one continental and one marine, were flown at the end of east-west pattern, shortly before turning back towards the airport. At such level, one should not expect to see striking differences between land and ocean parts, because boundary layer rather does not extend up there and the legs themselves are not many times longer as the distance to the ground.

In segment 4, quite a deep compact cloud was penetrated, with LWC reaching 1.5 g/m3 and droplets of mean and effective diameter of respectively around 16 and 20 microns. Full size distribution measured with Cloud Droplet Probe shows that there are even some droplets of diameter above 40 microns which means the cloud is capable of producing precipitations. This cloud is probably the one clearly visible in the satellite image. Wind velocity record indicates that it is being advected to the west onto the ocean.

Indeed, in the next leg at the same height, after about 1.5 hour, the cloud is found further to the west and extends quite far over the water. According to the notes taken by scientist onboard, the aircraft flew close to the cloud top. It is probably pushed down by a strong temperature inversion found at 1200 m in the second vertical sounding over ocean. The temperature inside the cloud is ~2 K lower than outside. Such pattern is a result of penetrating sharp inversion capping the cloud layer. The interface is not necessarily ideally flat and could be slightly tilted. LWC is much lower than before which means the cloud is dissipating due to mixing with warmer drier air from above or solar heating and consequent droplet evaporation. Average droplet sizes are not much smaller than before which might be the sign of inhomogeneous mixing.

Continental, segment 4 (leg_land 2)

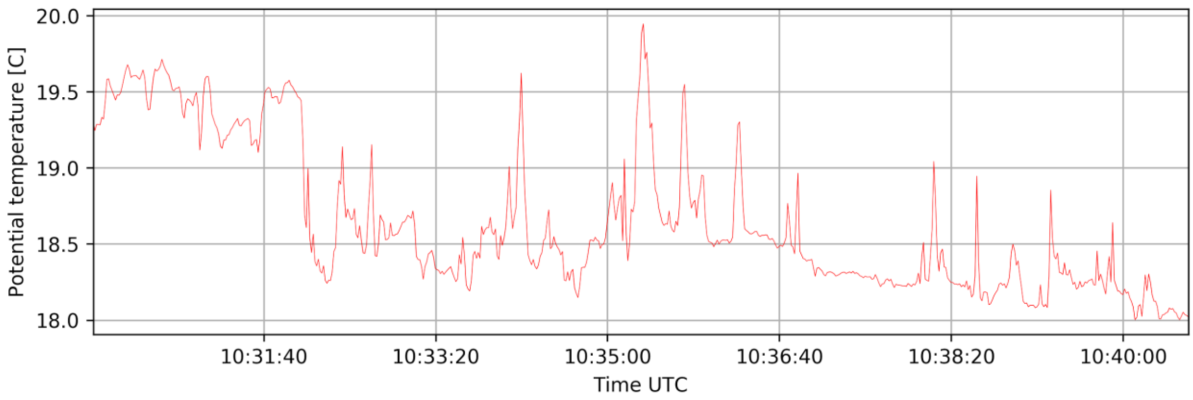

Figure 33.a. Segment 4. Potential temperature.

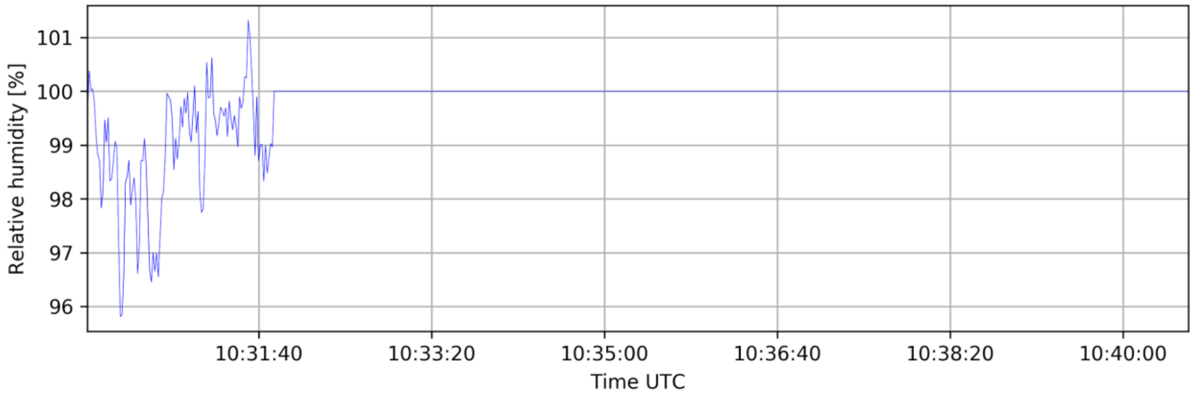

Figure 33.b. *Segment 4.* Relative humidity.

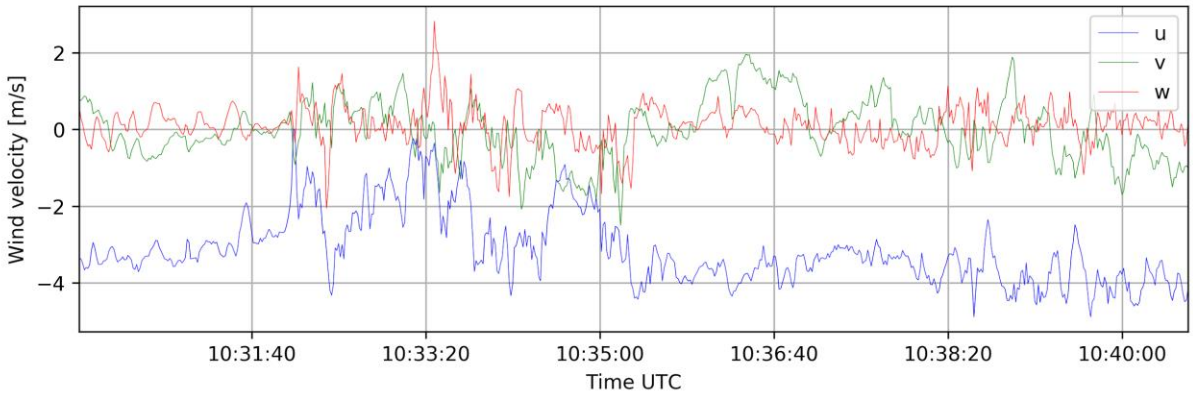

Figure 33.c. Segment 4. Wind velocity components.

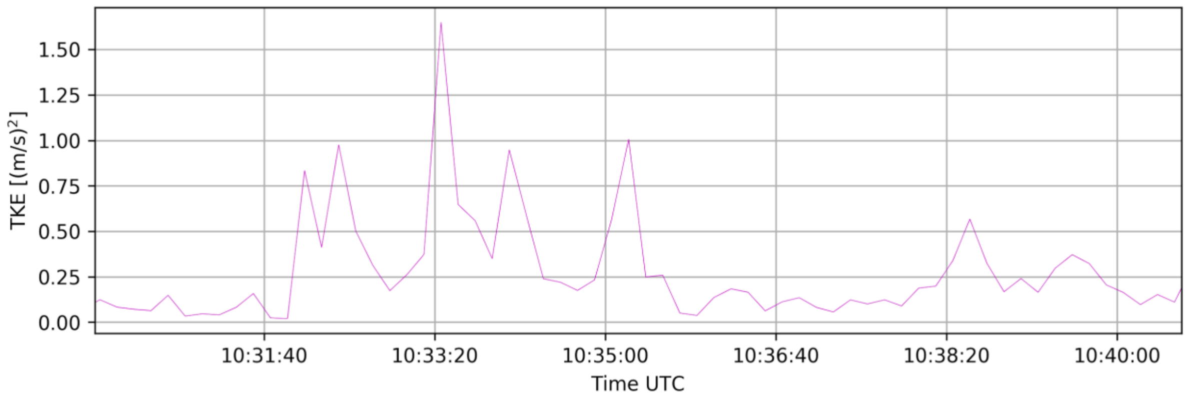

Figure 33.d. Segment 4. Turbulence kinetic energy.

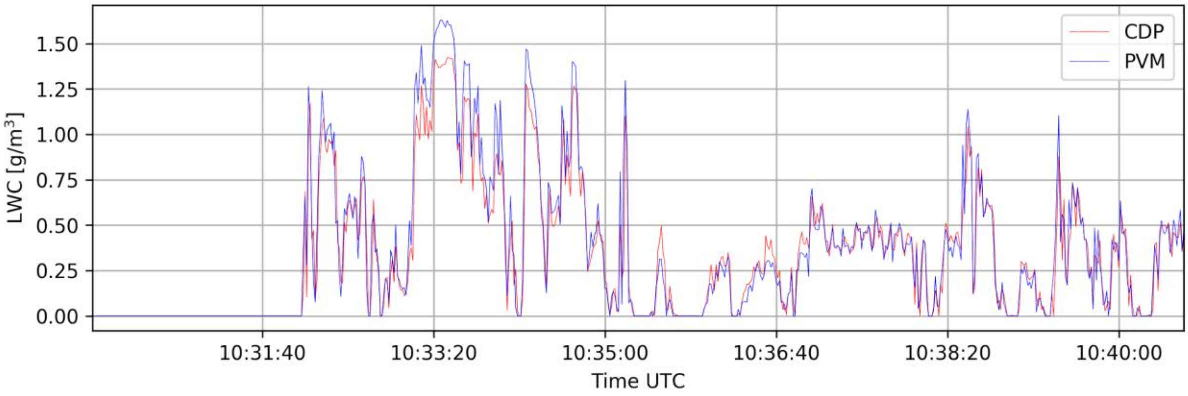

Figure 33.e. Segment 4. Liquid water content.

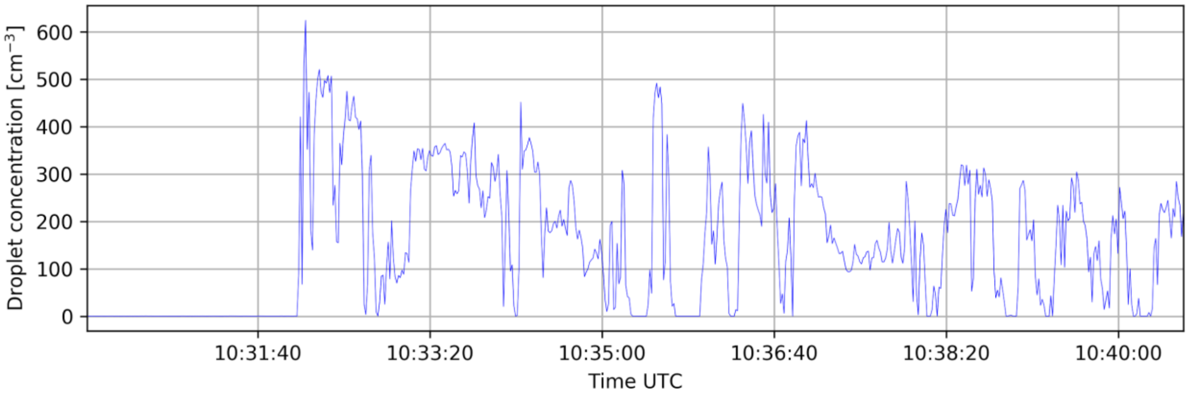

Figure 33.f. Segment 4. Cloud droplet number concentration.

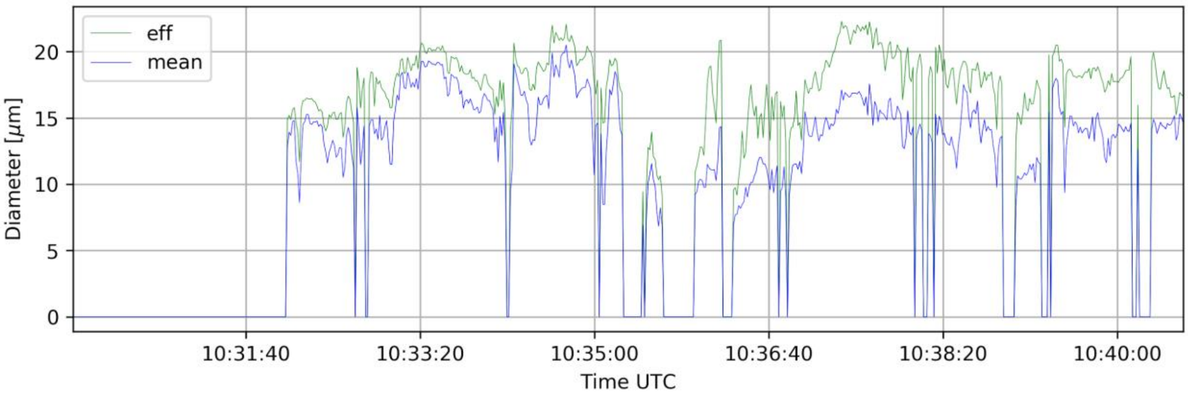

Figure 33.g. Segment 4. Mean and effective droplet diameter.

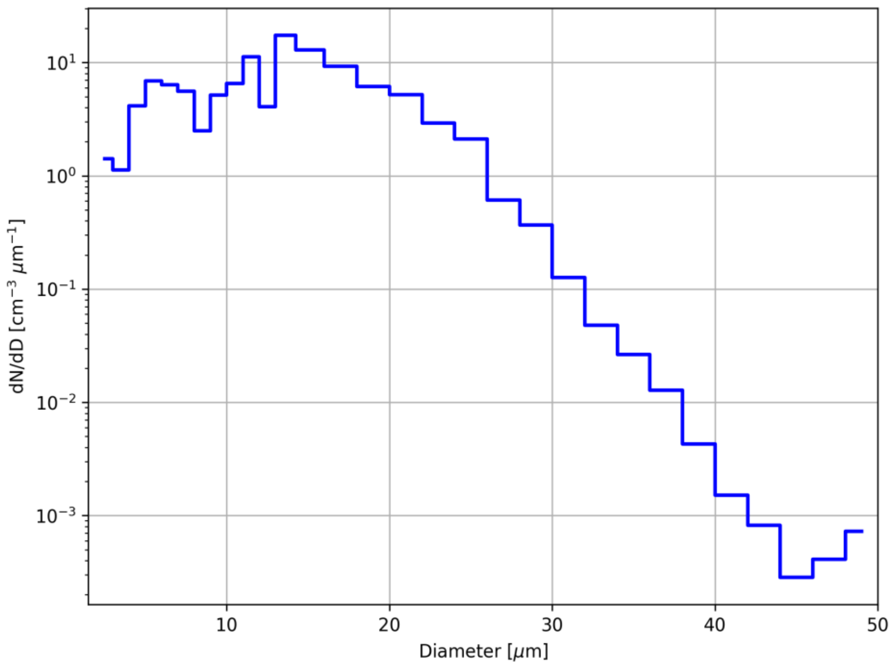

Figure 33.h. Segment 4. Droplet size distribution integrated over the leg.

Continental, segment 18 (leg_land5)

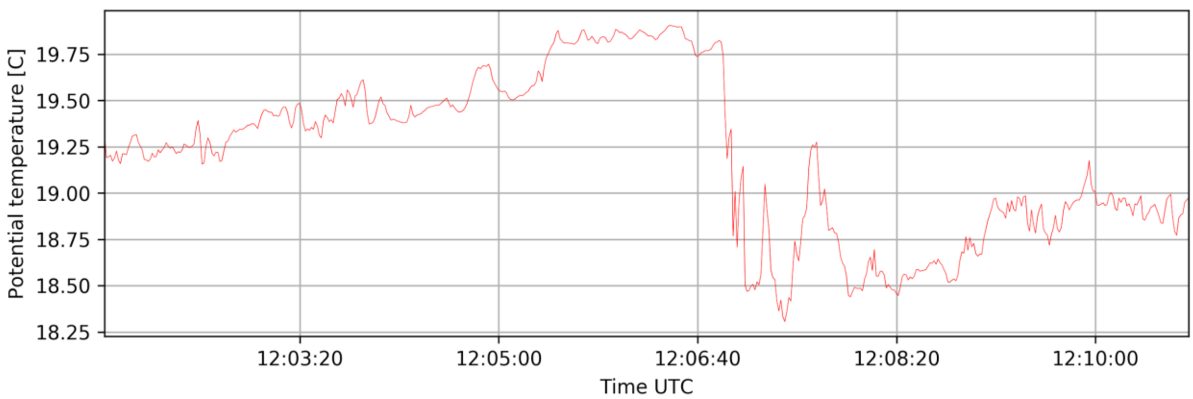

Figure 34.a. Segment 18. Potential temperature.

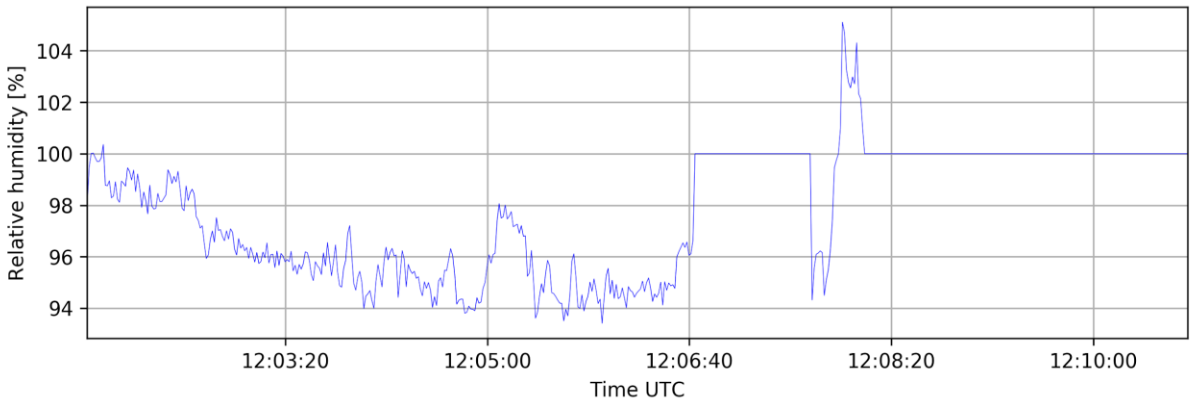

Figure 34.b. Segment 18. Relative humidity.

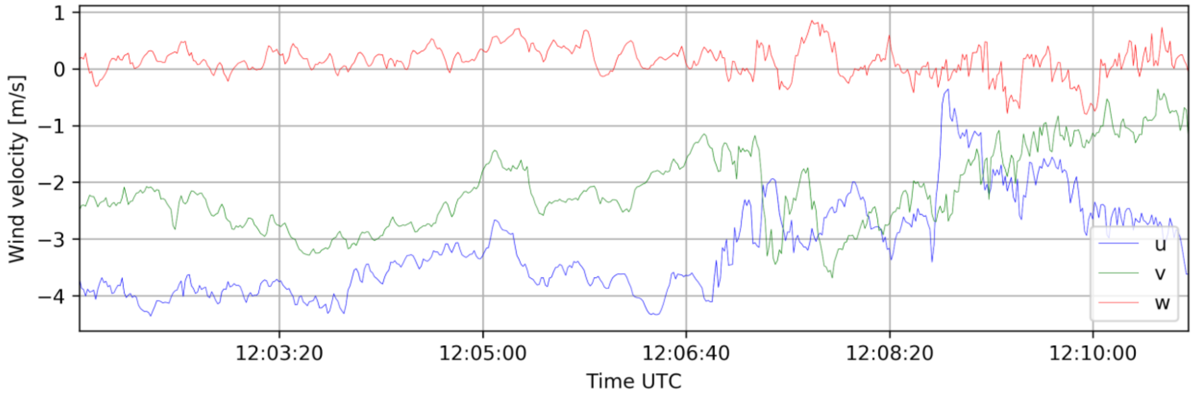

Figure 34.c. Segment 18. Wind velocity components.

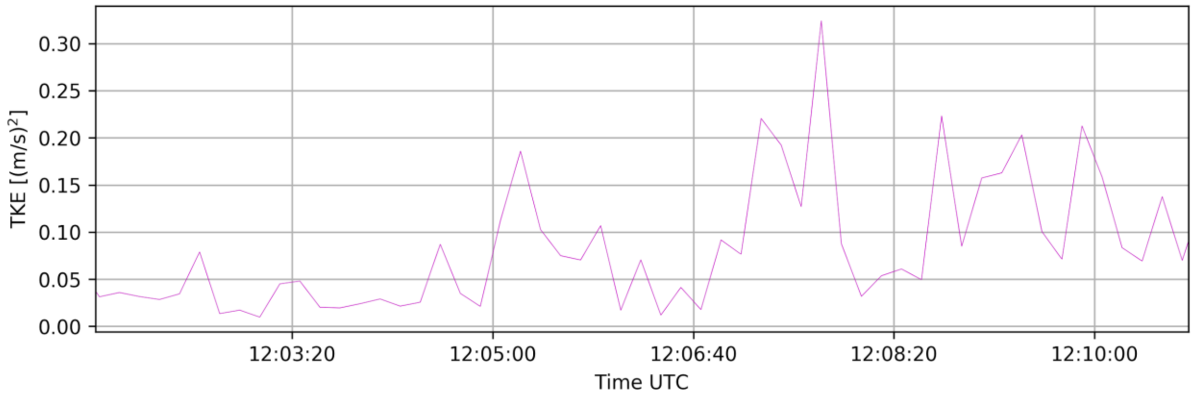

Figure 34.d. Segment 18. Turbulence kinetic energy.

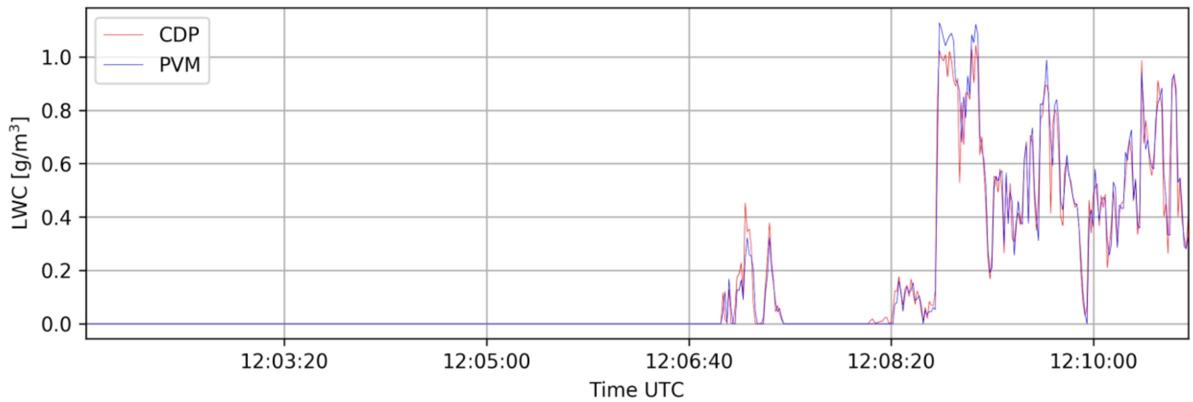

Figure 34.e. Segment 18. Liquid water content.

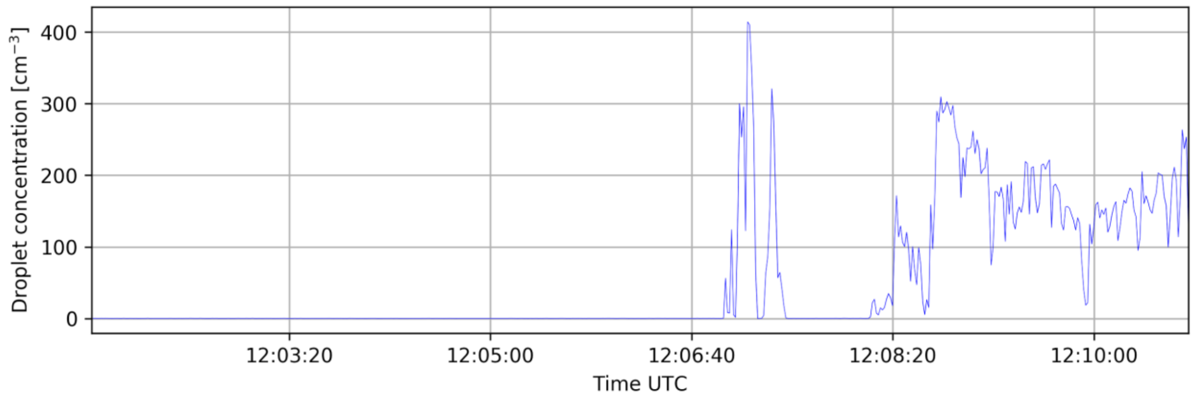

Figure 34.f. Segment 18. Cloud droplet number concentration.

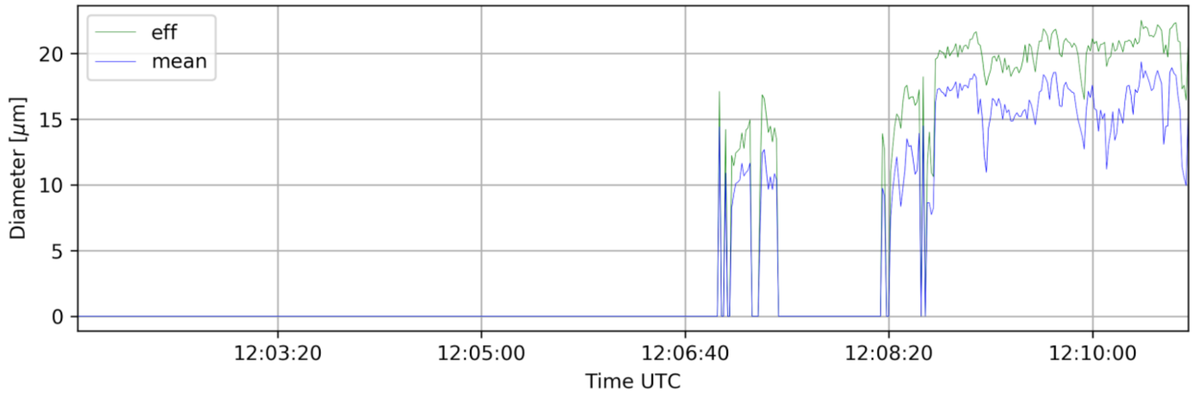

Figure 34.g. Segment 18. Mean and effective.

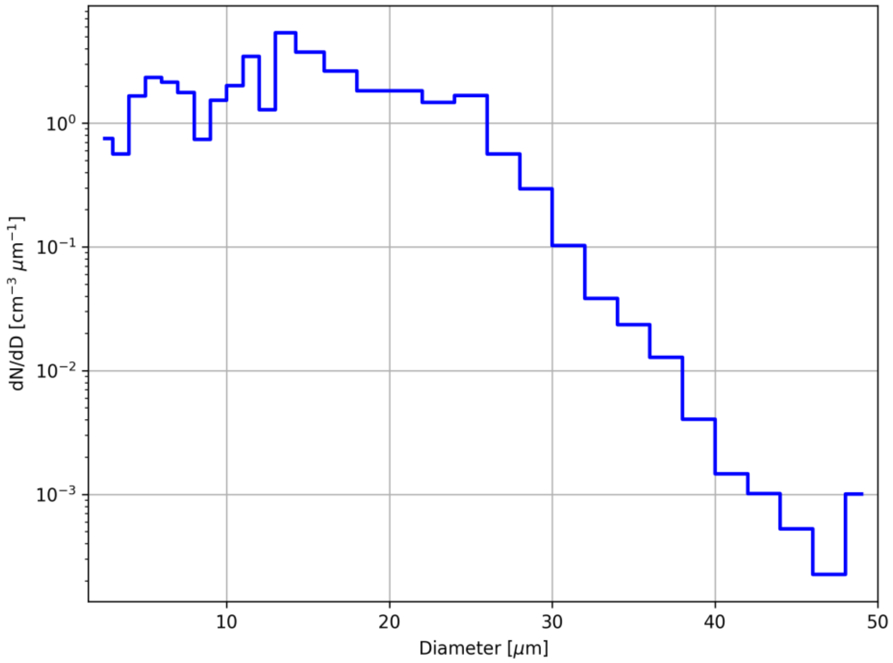

Figure 34.h. Segment 18. Droplet size distribution integrated over the leg.

<u>Marine, segment 19 (leg_oce5)</u>

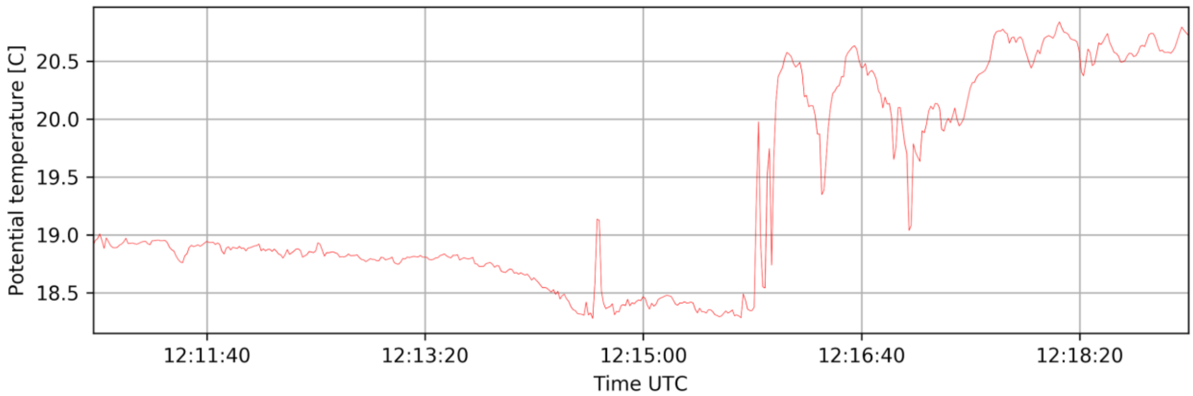

Figure 35.a. Segment 19. Potential temperature.

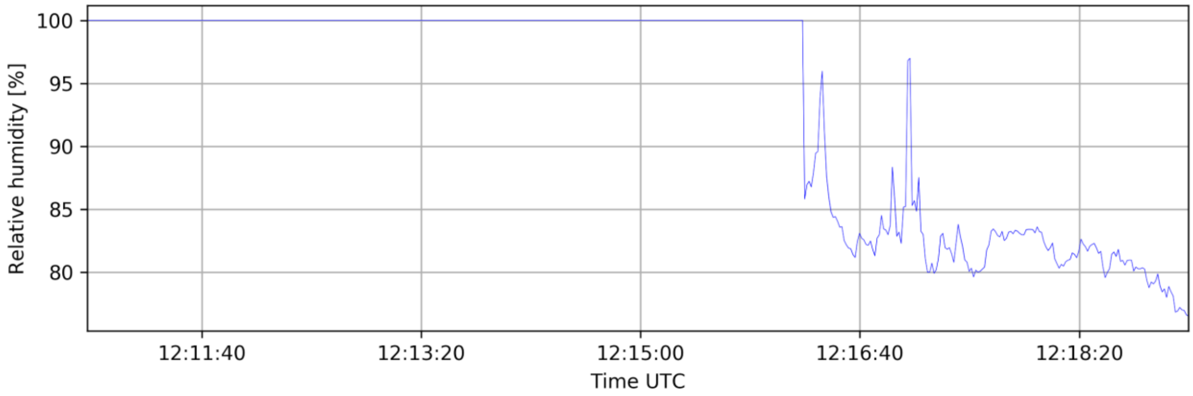

Figure 35.b. Segment 19. Relative humidity.

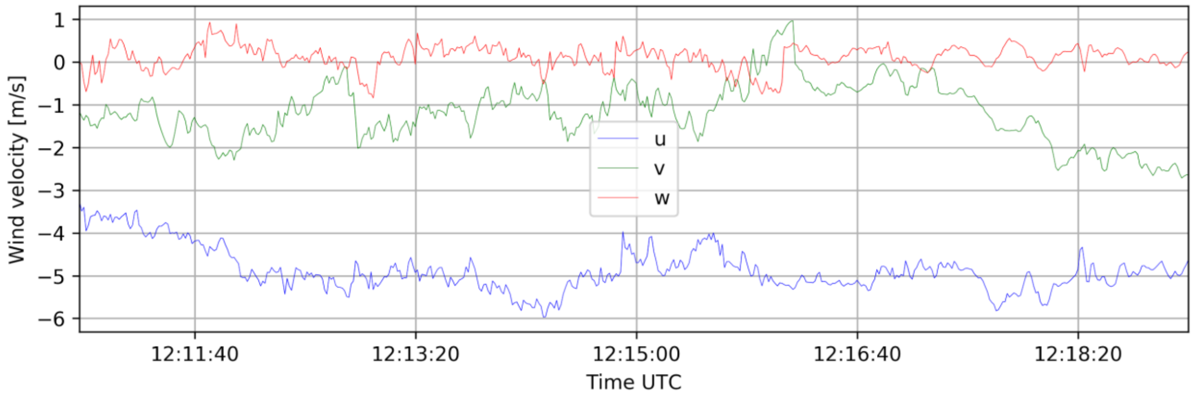

Figure 35.c. Segment 19. Wind velocity components.

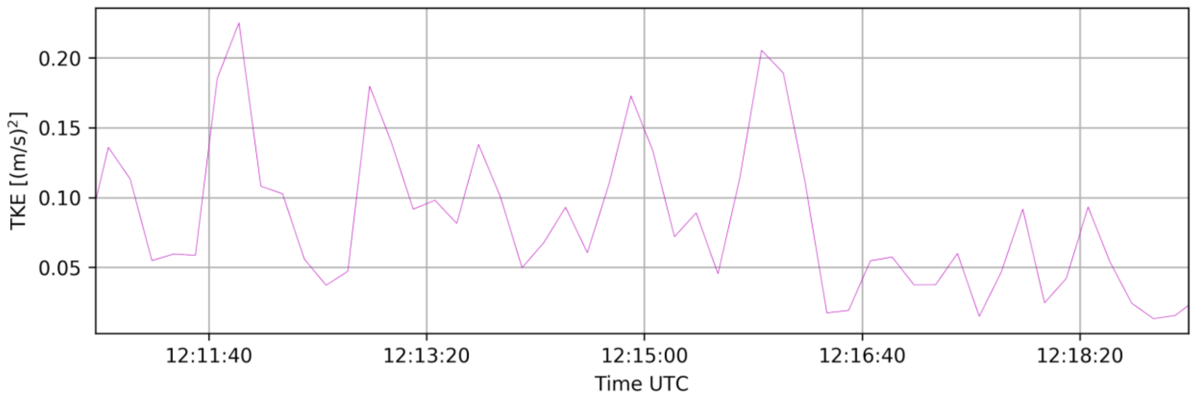

Figure 35.d. Segment 19. Turbulence kinetic energy.

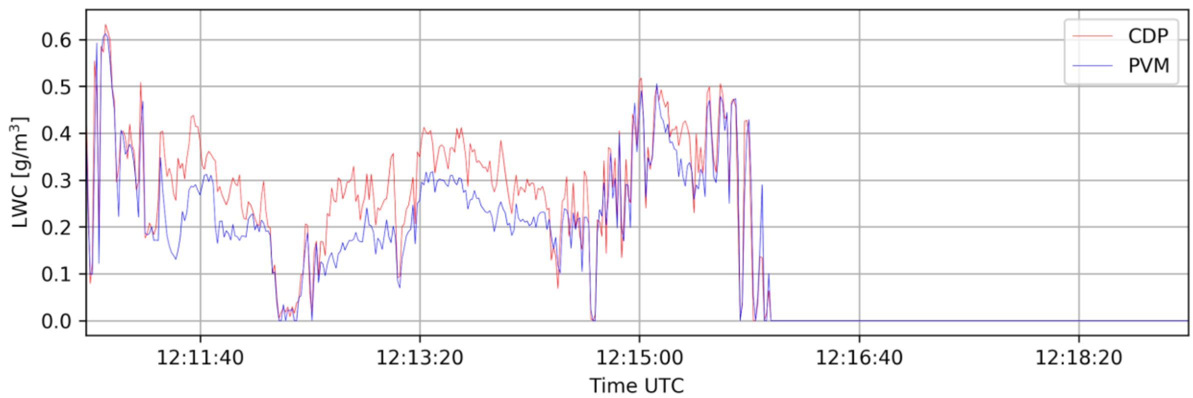

Figure 35.e. Segment 19. Liquid water content.

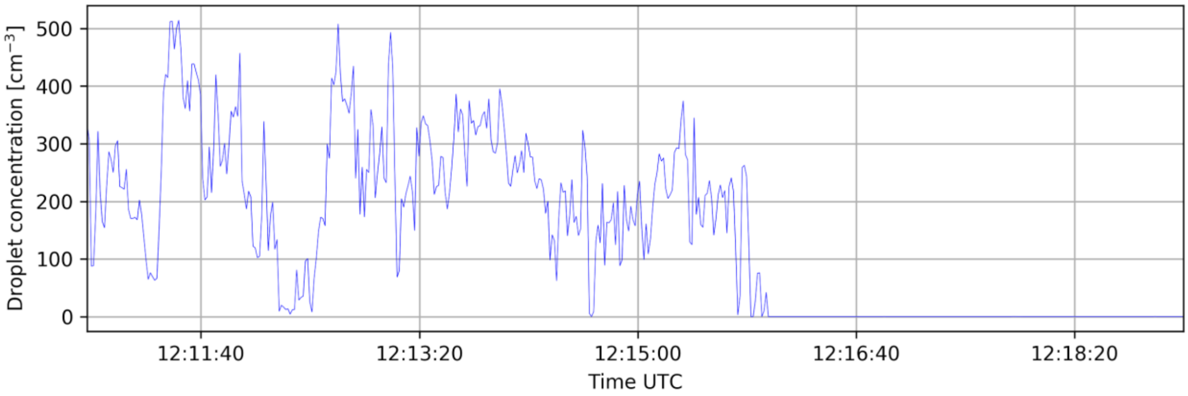

Figure 35.f. Segment 19. Cloud droplet number concentration.

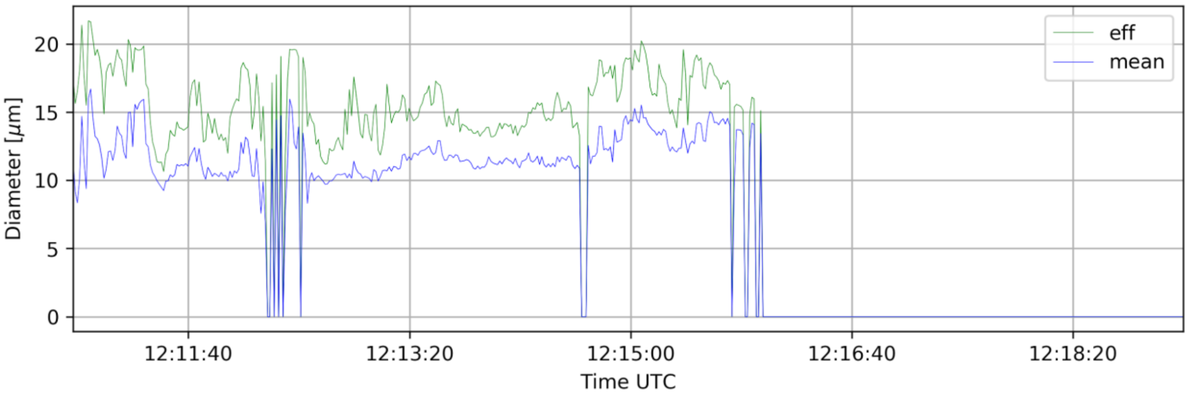

Figure 35.g. Segment 19. Mean and effective droplet diameter.

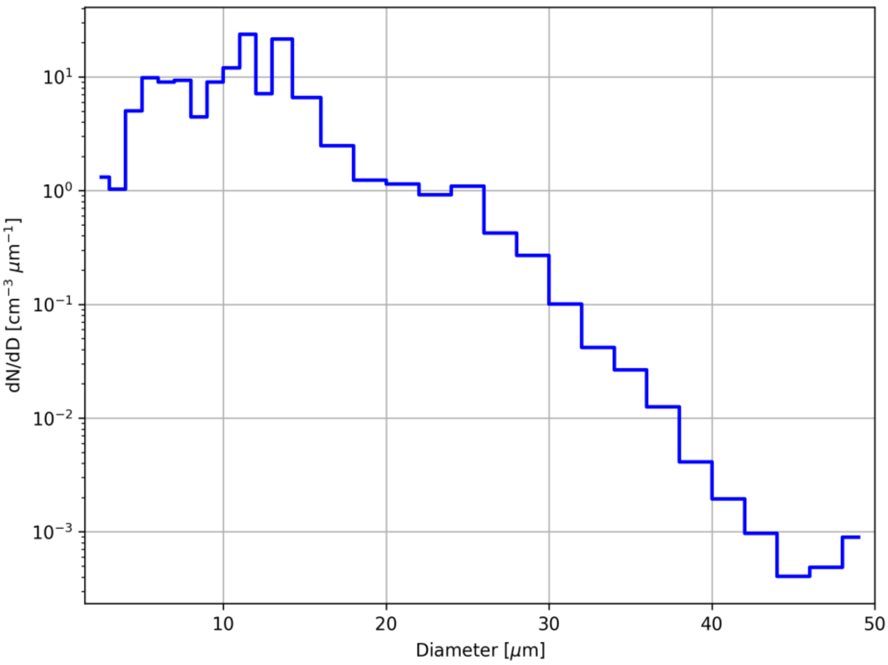

Figure 35.g. Segment 19. Droplet size distribution integrated over the leg.

7.3. CHEMISTRY COMPOSITION PROFILES

Just before summing up all the results in the conclusions section, we wanted to briefly show some results regarding the chemistry composition profiles of the atmosphere during our research flight. Using the measurements taken during the whole flight, 100 m bin averages of CO_2, O_3, CO and CH_4 were calculated, obtaining the profiles shown in figure 36. Must be noted that only sea/land separation has been applied to the data, so averages correspond to data measured at different locations along the flight path and at different times (spatial and temporal averages). The most interesting profile is probably the CO_2 average profile, in which the average height of the top of the BL can be guessed as a sharp drop in CO_2 concentration: occurring at a higher altitude over land than over ocean. That matches our findings of a more developed BL over land. From the CH_4 profile one can notice different roles played by the land and ocean as sources. The O_3 concentration increases with altitude over the both surfaces, but slightly higher concentrations are found over the sea. Regarding CO, the measured profiles are very noisy, which matches with the information from CO spectra.

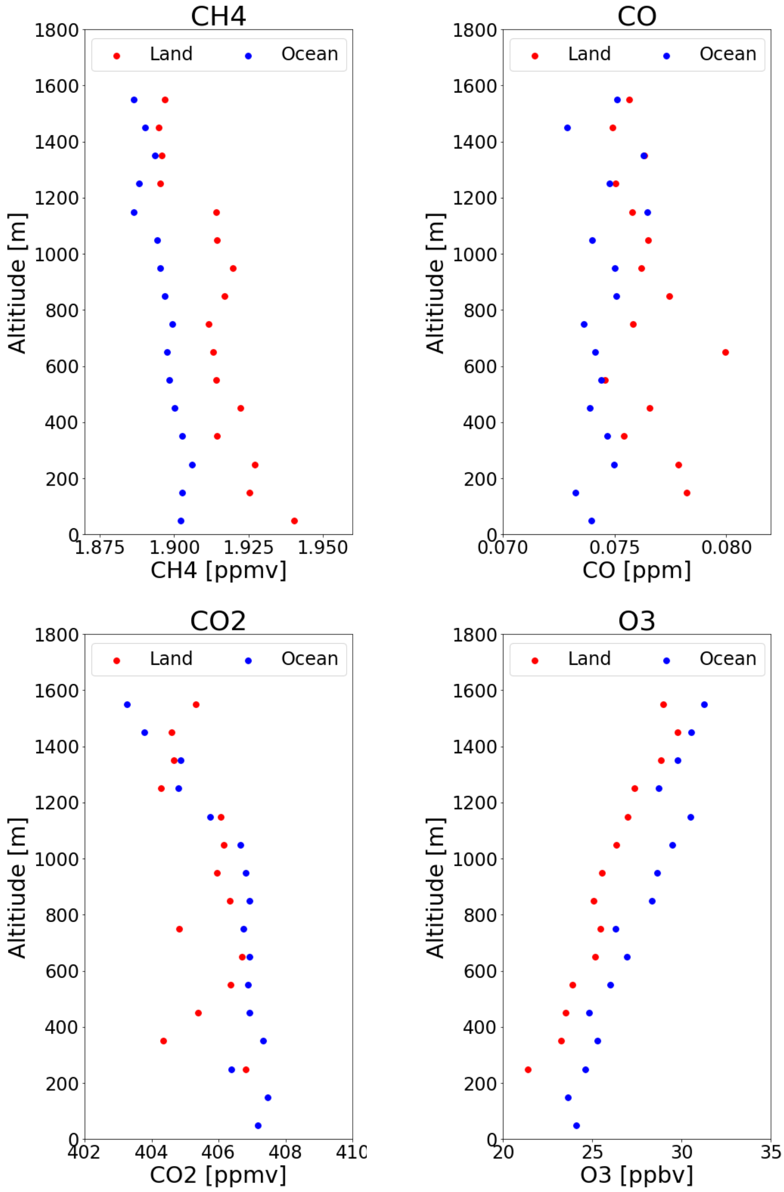

Figure 36. Vertical profiles of chemical compounds concentration: comparison between land and ocean.

8. CONCLUSIONS

The aim of our research flight was to study the differences between the marine boundary layer and the terrestrial boundary layer given the particular site. This report has focused on studying these differences through the analysis of several atmospheric aspects: dynamics, thermodynamics and cloud microphysics. The designed flight plan was successfully followed the day of the research flight (28 June 2017), and it basically consisted of east-west horizontal legs half over ocean and half over sea. The minimum altitude flown over sea was 65 m, and 405 m over land due to the presence of clouds and topography. However, it was possible to fly inside the ABL over both surfaces, which was not taken for granted during the weather briefing held on the same day. Additionally, a few soundings were also made as part of the flight plan in order to have a picture of the vertical structure of the atmosphere at different times of the flight. The highest leg performed was at 1230 m altitude.

In order to analyze the information recorded during the flight, data was separated into segments corresponding to horizontal legs and profiles over land and over sea. The analysis of the **vertical structure** of the lowest part of the atmosphere (over ocean and over sea) and its temporal evolution was made using profile-type segments distant in time for both surfaces. The vertical structure has been studied in terms of dynamics, thermodynamics and also microphysics (wind, turbulence kinetic energy, potential temperature, humidity, among others), providing useful information about stability, different layers and the top ABL itself.
Regarding the vertical structure of the lower atmosphere over land, different layers were identified and they changed during the 2-hour flight. The top of the BL at the beginning of the flight was detected at 300 m approximately (not very developed due to considerable cloud cover and only few hours after the sun rising), but adjacent to a stable middle layer (up to 900 m) that could have been the residual BL from the previous day. After two hours, convection processes were more present, being responsible for the mixing of the initial lowest layer and the middle one. Due to that, the top of the boundary layer could be identified then at around 900 m. At higher altitudes (above 900 m approx.) a complex cloud layer (decoupled from the surface) was present. It either consisted of independent cloud layers or was not horizontally homogeneous.
Over ocean, the vertical structure observed in the beginning of the flight was way more complex, containing up to 5 different layers. The lowest layer, corresponding to the well-mixed boundary layer extended only up to 150 m (lower than the continental boundary layer due to less convection from the surface) and a second layer probably corresponding to a residual BL from previous days was detected above. The same structure was observed for the continental vertical profile at the beginning of the flight. Other three more layers were detected, the highest one corresponding to a homogeneous cloud layer with cloud base at 1200 m. The time evolution of the marine boundary layer was similar to what was observed for the continental. The BL extended up to 400 m because of the mixing of the two first layers encountered initially. At the top of this developed BL a shallow cloud is observed. The remaining layers appear now as a unified layer from 400-1100 m, capped with a strong temperature inversion and drop in humidity.
For both surfaces we observed a more stratified structure at the beginning, with presence of at least an intermediate layer that could be a residual BL from the past days. After 2 hours, the convection mechanisms activated and the BL extended including those intermediate residual BL. The different extension of the BL over land and ocean was also detected by

analyzing the chemistry composition profiles. Particularly, in the CO_2 a sharp drop in concentration is observed where the top of the boundary layer was identified to be.

The analysis of the **horizontal legs** was made in terms of the same physical quantities as the profiles, but comparing adjacent segments (land/sea) at the same level (altitude) to look at the transition between zones with different characteristics. Only a three common levels are available over both surfaces (~405 m, ~740 m, and ~1230 m), while the lowest levels (~65 m and ~165 m) were only performed over the sea (due to good visibility). None of the common levels are simultaneously inside the marine and the continental boundary layer. The lowest common level (~405 m) corresponds to the top of the marine BL at the end of the flight.
First level (marine only, 65 m) was reached twice during the flight (beginning and close to the end) and differences were detected: increase of horizontal wind and TKE, indicators of the developing of the BL. This level was the only one completely inside the marine BL. The second level (marine only, 165 m) was located in the surroundings of the top of the BL by the time it was performed, so it presented similar properties as the well-mixed layer below.
During the third level (marine and continental, 405 m) drops in temperature and humidity are detected when going inland, as well as an increase in zonal wind. However, the transition between continental and marine is not sharp, but differences in wind fluctuations and TKE were observed.
In the higher levels, the difference between marine and continental part of the leg was less evident, even though more mixing is always present over the land. Clouds were encountered during the ocean part of the fourth level leg (740 m), with higher LWC than at the previous level. While flying into the island, droplet number concentration grows but mean droplet sizes decrease.
It was hard to see differences in the last level studied (1230 m), which was higher than the top of the BL over both surfaces. Nevertheless, interesting cloud information was obtained from these legs. A cloud capable of producing precipitations was penetrated (probably the one visible in the satellite image) and it was checked that this cloud was the result of the advection to the west: easterly winds were recorded and because this cloud was found further to the west when performing a same altitude leg near the end of the flight.

Summarizing, we only could see major differences between marine and continental atmospheric situation at the lowest common level studied (405 m), altitude in which the convection processes were active over land and slightly present over ocean. There, the vertical structure has a chance to be influenced by the surface beneath. At higher levels, differences fade and large scale mechanism take over the leading role.

ACKNOWLEDGEMENTS

The research leading to these results has received funding from the European Facility for Airborne Research in Environmental and Geo-sciences (EUFAR), a project of the EC's 7th Framework Programme (FP7/2014-2018) under grant agreement n°312609. The authors are wish to express their deep gratitude to the EASI organizing committee and trainers as well as the SAFIRE pilots and technical staff for the support during the course and the research flight.